UNIVERSITY OF CALIFORNIA SAN DIEGO

Identification and expression of a novel urethanase enzyme and development of a urethanase assay

A thesis submitted in partial satisfaction of the requirements

for the degree Master of Science

in

Chemistry

by

Ariel Canaan Schreiman

Committee in charge:

Stephen P. Mayfield, Chair
Michael D. Burkart
Robert S. Pomeroy

2021

The thesis of Ariel Schreiman is approved, and it is acceptable in quality and form for publication on microfilm and electronically.

University of California San Diego

2021

TABLE OF CONTENTS

LIST OF ABBREVIATIONS

PLA – Polylactic acid

PET – Polyethylene terephthalate

PU – Polyurethane

DNA – Deoxyribose nucleic acid

MIN – M9 minimal media with added nutrients

LB – Lysogeny broth

PDA – Potato dextrose agar

PCR – Polymerase chain reaction

Ps – Pseudomonas bacterial isolate from compost

Rh – Rhodococcus bacterial isolate from soil

MiGA – Microbial Genomes Atlas

ANI – Average nucleotide identity

BPMSF – UCSD Biomolecular and Proteomics Mass Spectrometry Facility

Impranil – Covestro Impranil®DLN SD

MDBC – Methylene bisphenyl dicarbamic acid dibutyl ester

IPTG – Isopropyl-β-d-thiogalactopyranoside

6xHis – Hexahistidine tag

NEB – New England Biolabs

LB+Kan – LB agar plates with 50 ug/mL kanamycin

PBS – Phosphate-buffered saline

BSA – Bovine serum albumin

DMSO – Dimethylsulfoxide

NADH – β-nicotinamide adenine dinucleotide

MDI – Methylene diphenyl diisocyanate

MDA – 4,4'-Methylenedianiline

Fluorescamine – 4-phenylspiro[furan-2(3H), 1’-phthalan]-3,3’-dione

GCMS – Gas Chromatography–Mass Spectrometry

HPLC – High Performance–Liquid Chromatography

EtOAc – Ethyl acetate

MSTFA – N-Methyl-N-trimethylsilyl trifluoroacetamide

LCMS – Liquid Chromatography–Mass Spectrometry

LIST OF FIGURES

LIST OF TABLES

PREFACE

This thesis was completed with the partnership and funding of Algenesis Materials in order to further understand the properties of polyurethane materials and their potential as a biodegradable polymer, helping to address the urgent need for plastics which will biodegrade completely instead of remaining as microplastics in the environment. Research was performed in collaboration with researchers in the UCSD Department of Chemistry & Biochemistry, the UCSD Biological Sciences Division, and Algenesis Materials.

ACKNOWLEDGEMENTS

I would like to acknowledge Dr. Stephen Mayfield for his mentorship over the past four years during which I have learned so much, and especially for the opportunity to complete a Master's degree at UCSD this past school year. I would also like to thank Dr. Michael Burkart and Dr. Robert Pomeroy for their support and guidance throughout my research.

I also want to recognize my amazing friends and colleagues Natasha Gunawan, Marissa Tessman, and Anthony Berndt who have been a constant inspiration and have provided invaluable suggestions. I have learned so much from you all and could not have accomplished any of this without you. And thank you to Ryan Simkovsky and Majid Ghassemian for your technical advice.

This research was performed in partnership with Algenesis Materials through the funding of a DOE Small Business Innovations and Research Phase II grant (DE-FOA-0002156, No. 13078829).

Chapter 1, in part, is a reprint of the material as it appears in "Rapid biodegradation of renewable polyurethane foams with identification of associated microorganisms and decomposition products" in Bioresource Technology 2020. Gunawan, Natasha R.; Tessman, Marissa; Schreiman, Ariel C.; Simkovsky, Ryan; Samoylov, Anton A.; Neelakantan, Nitin K.; Bemis, Troy A.; Burkart, Michael D.; Pomeroy, Robert S.; Mayfield, Stephen P. The thesis author was an investigator and third author of this material.

Chapter 2, in part, is a reprint of the material as it appears in "Rapid biodegradation of renewable polyurethane foams with identification of associated microorganisms and decomposition products" in Bioresource Technology 2020. Gunawan, Natasha R.; Tessman, Marissa; Schreiman, Ariel C.; Simkovsky, Ryan; Samoylov, Anton A.; Neelakantan, Nitin K.;

Bemis, Troy A.; Burkart, Michael D.; Pomeroy, Robert S.; Mayfield, Stephen P. The thesis author was an investigator and third author of this material.

Chapter 4, in part, is a reprint of the material as it appears in "Rapid biodegradation of renewable polyurethane foams with identification of associated microorganisms and decomposition products" in Bioresource Technology 2020. Gunawan, Natasha R.; Tessman, Marissa; Schreiman, Ariel C.; Simkovsky, Ryan; Samoylov, Anton A.; Neelakantan, Nitin K.; Bemis, Troy A.; Burkart, Michael D.; Pomeroy, Robert S.; Mayfield, Stephen P. The thesis author was an investigator and third author of this material.

ABSTRACT OF THE THESIS

Identification and expression of a novel urethanase enzyme

and development of a urethanase assay

by

Ariel Canaan Schreiman

Master of Science in Chemistry

University of California San Diego, 2021

Professor Stephen P. Mayfield, Chair

Plastic recycling is a difficult process because of the variability in starting material and contamination with food and other chemicals. Very little of current plastic production comes from recycled material. In addition, many plastics are sourced from petroleum, which is nonrenewable and releases toxic chemicals into the environment. However, more plastic is produced each year.

To solve this problem, it is necessary to devise new methods for recycling plastic. In this thesis, two bacterial isolates are shown to grow using polyurethane foam as their sole carbon source, their genomes sequenced, and proteomics methods used to identify potential urethanase enzymes. Next, enzymes were expressed in *E. coli* and tested using an Impranil assay. Finally, two novel urethanase assays were developed, a fluorometric one using a synthesized urethane substrate, and a mass-spectrometry one directly using particles of polyurethane foam. Genome sequencing of the two isolates produced assembled draft sequences, one of which was fully polished and circularized, and the other which was polished but did not circularize. Proteomics identified a large number of hydrolase enzymes overexpressed when isolates were grown in polyurethane media, of which nine were selected as likely urethanase candidates. One enzyme was successfully expressed, but it was a slightly truncated variant and only expressed in low quantities. All three enzyme assays were tested and resulted in promising proof-of-concept results.

Chapter 1: Introduction

1.1 Current State of Plastic Use and Production

Over the past 50 years, humans have generated over 6 billion metric tons of plastic waste. Of this, only about 9% was recycled, 12% was incinerated, and 79% was left to accumulate in landfills or the natural environment. If current production and waste management trends continue, roughly 96 billion tons of plastic waste will be in landfills or in the natural environment by 2050 (Geyer, Jambeck, and Law 2017). In addition to the large carbon footprint and water consumption of petroleum and plastic production, the overwhelming majority of plastics endure in the environment for hundreds of years, where they can degrade into microplastics that are first consumed by primary consumers, but eventually move up the food chain, interfering with metabolism, reproduction, and increased mortality rates (Anbumani and Kakkar 2018; Betts 2008; Masnadi et al. 2018; Moore 2008; Sun et al. 2018). The adverse effects of petroleum-based plastic production on health and the environment are well-documented. Pollution emitted during petroleum drilling, refining, and waste management practices leads to cardiovascular disease and respiratory conditions, whereas toxic emissions or leachables from degrading plastics act as endocrine disruptors and can cause cancer (Azoulay et al. 2019). Given these deleterious environmental effects, there is a need for plastics that can be sourced from renewable feedstocks and can undergo biodegradation at the end of their useful life.

1.2 Biodegradation of Plastic

Biodegradation is the process where a material breaks down into smaller pieces which are eventually decomposed by microorganisms in the environment and the constituent chemicals metabolized for energy production or growth. Biodegradation occurs through a series of steps where the plastic is first colonized by microorganisms, then these organisms chemically break

down the polymer structure into smaller oligomers, and finally the organisms metabolize these chemicals into carbon dioxide or cellular components (Michael Thomas Zumstein et al. 2018). This is not the same process as the formation of microplastics, where a plastic material breaks down into smaller, but chemically similar, pieces through physical processes and photooxidation (Yashchuk, Portillo, and Hermida 2012). Microplastics are now known to have health and environmental concerns and can concentrate in the food chain; these small particles can concentrate plastic additives and persistent organic pollutants (Andrady 2017).

Plastics have varying rates of biodegradation based on many factors, most notably their chemical structure. Some plastics have an entirely C–C backbone while others contain heteroatoms of oxygen or nitrogen as part of the backbone; those which incorporate heteroatoms can undergo hydrolysis while those with only carbon bonds typically require more difficult oxidative methods to initiate biodegradation. The other important factor for biodegradation is the environment around the plastic waste. Sunny, warm, aerobic environments typically afford faster biodegradation than anaerobic, colder, or dark environments (Ali et al. 2021). Similarly, plastics in soil and compost typically degrade quicker than plastics in the ocean. An excellent example is polylactic acid (PLA) plastic, which biodegrades in compost; however, it does not biodegrade in the ocean (Pradhan et al. 2010; Anderson and Shenkar 2021). To study the biodegradation of plastics in various environments, there exist standardized methodologies created by organizations including ASTM International and the International Organization for Standardization (Michael T. Zumstein et al. 2019).

Some biodegradable plastics are already in use, most notably PLA plastic. These materials are particularly useful for food packaging, agricultural, and medical applications. However, there are several problems with using these plastics: they may have lackluster physical or chemical

properties compared to alternatives, degrade too quickly, and may not be biodegradable in all environments (Iwata 2015). Because of these limitations, it is not currently possible to replace all nonbiodegradable plastics with biodegradable materials.

1.3 Advances in Plastic Recycling

While studying biodegradation is useful for understanding the impact of plastic materials on the environment, it is desirable to engineer methods to recycle existing plastics, reducing the need for virgin plastic production. Specific kinds of plastics called thermoplastics can be melted and reshaped, while others called thermosets, react into a specific shape and cannot be reformed into a new shape through melting (Amobonye et al. 2021). Thermoplastics can be mechanically recycled by melting and reforming, however there are many difficulties in this process due to chemical contaminants from plastic use and physical degradation of the plastic over time, resulting in lower quality materials. Lower quality recycled plastic often must be mixed with virgin plastic to create useful products (Eriksen et al. 2019). Polyethylene terephthalate (PET) plastic has many advantages over other plastics when recycled, but nevertheless it is typically mixed with virgin material during the recycling process (Welle 2011). Thermosets are even more difficult because they cannot be melted and reformed, though some recycling processes have been developed (W. Yang et al. 2012; Asaro et al. 2018).

An alternative possibility is chemical depolymerization, where plastic is chemically decomposed into its original monomers, then these are purified and reacted to create a new plastic. This methodology shows great promise because of the wide applicability of this technique for creating value-added final products (Thiounn and Smith 2020). Enzymes in particular are interesting potential catalysts for chemical depolymerization due to their specificity and ability to operate at lower temperatures. Enzymes could improve the environmental sustainability of plastic

recycling, however there are still a number of technical challenges to solve: stable C–C bonds require oxidative mechanisms to be broken, the high molecular weight makes plastics hydrophobic and difficult to access by enzyme, and the crystallinity of many materials which further limits enzymatic activity (Wei and Zimmermann 2017). While many plastics have been demonstrated to biodegrade in the presence of certain organisms, and many enzymes have been identified which can depolymerize various types of plastic, most enzymes lack the necessary specificity and reaction rate to commercialize this technology (Amobonye et al. 2021; Wei and Zimmermann 2017). PET plastic has recently been enzymatically depolymerized and resynthesized in a proof-of-concept experiment which demonstrated the feasibility of this concept. Authors used computer-aided enzyme engineering to optimize the enzyme used in the experiment, which resulted in high depolymerization rates. When the authors purified the monomers and resynthesized PET plastic, they found no significant differences from petroleum-derived PET (Tournier et al. 2020).

1.4 Polyurethanes

Among the wide variety of materials used to make plastics, polyurethane (PU), especially polyester PU, have the potential to be renewably sourced and subsequently biodegraded (Howard 2002; Nguyen et al. 2010; Sonnenschein 2021). Unlike many other polymers, they can be synthesized from a diverse set of monomers. A typical PU contains repeating urethane bonds produced by linking a polyol, a hydrocarbon with at least two hydroxyl groups, and a diisocyanate, but the identity of the polyol or the molecule carrying the isocyanates can vary widely in composition and size, making PU an ideal canvas for innovation in renewable and biodegradable plastics.

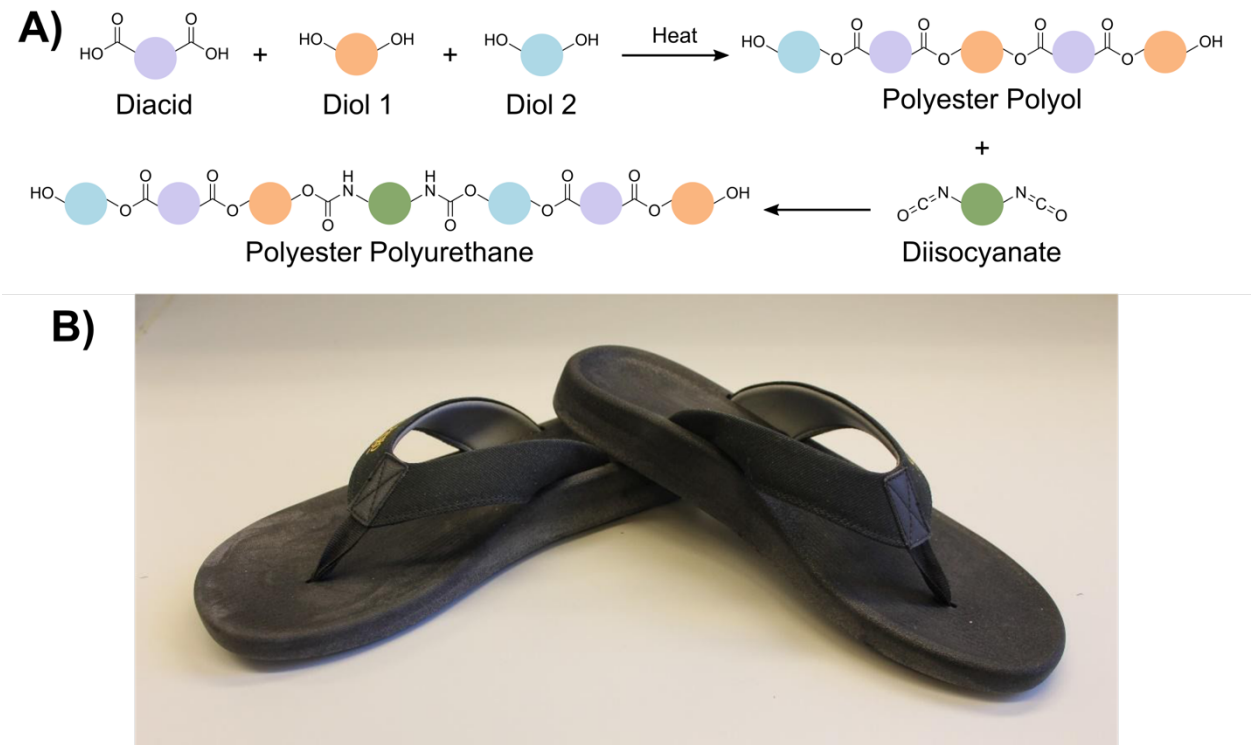

Figure 1: A) General synthesis of polyester PU from requisite monomers. B) Prototype flip-flop produced by Algenesis from bio-based polyester PU foam.

Previous studies have demonstrated that polyester PU, in which the polyol contains repeating ester linkages (Figure 1), can degrade under various chemical and biological conditions through cleavage of the ester bonds (Osman et al. 2018). Several chemical methods, including hydrolysis and glycolysis with alcohols, are proven to cleave polyesters (Sheel et al. 2018; Wu et al. 2003). In previous literature, various bacteria and fungi have been found to degrade polyester PU through the use of esterase, urease, amidase, and protease enzymes (Magnin et al. 2019). PU biodegradation is largely controlled by the activity of secreted or surface-bound enzymes and their ability to access the soft segment ester groups (Santerre and Labow 1997). In particular, esterase enzymes, such as lipases and LC cutinases, have been shown to hydrolyze polyester PU bonds (Howard 2002). However, the possibility of using enzymes to fully depolymerize PU remains understudied.

1.5 Experimental Design

In this thesis, the enzymatic depolymerization of PU is studied (Figure 2). First, soil and compost inoculum were serially passaged in media containing PU foam as the sole carbon source and surviving strains of bacteria were isolated. Bacterial strains were then cultured individually in media containing PU foam, and growth was monitored to identify strains which could use PU as their sole carbon source. Next, two of these isolates were selected for further study. First, genomic DNA was purified, sequenced, assembled, and annotated to determine the genes present in each strain. Then, both strains were grown in minimal media containing either dextrose or PU as the carbon source and mass spectrometry was used to identify which proteins were upregulated during growth on PU. Across the two organisms, nine enzymes were identified as potential urethanases due to homology with hydrolase enzymes and high expression in PU-containing media. One of these enzymes was expressed and assayed for esterase activity with a standard method. In addition, two novel enzymatic assays were developed and validated: a fluorescence-based urethanase assay and a PU foam degradation assay based on mass-spectrometry.

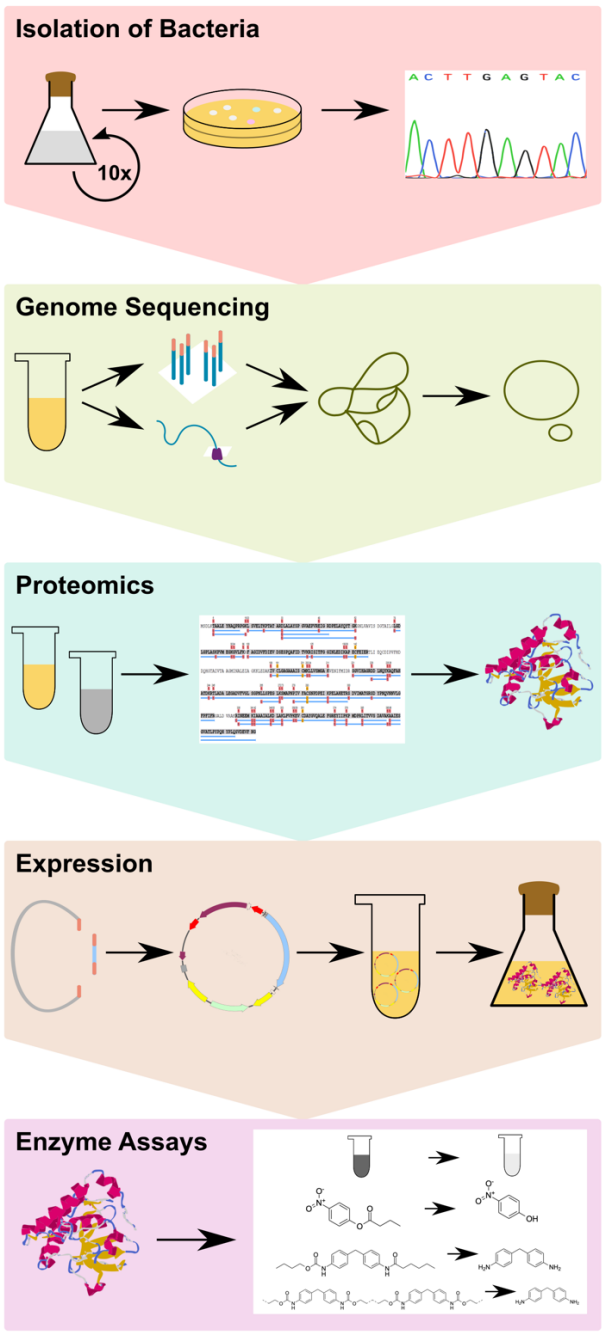

Figure 2: Diagram of the experimental design in this thesis for identifying and testing urethanase enzymes. Major steps depicted, in order, are: (Isolation of Bacteria) inoculation and serial passaging of PU media, plating onto rich media, identification of isolated bacteria, (Genome Sequencing) purification of genomic DNA from isolated bacterial cultures, sequencing genomic DNA, assembly of sequencing reads, polishing and circularization of assembly, (Proteomics) incubation of bacterial isolates in two culture conditions, mass spectrometry of proteins, structure and function prediction of identified proteins, (Expression) synthesis of vector and gene of interest, assembly of plasmid, transformation into *E. coli*, expression of protein, and (Enzyme Assays) incubation of expressed enzyme with selected assays.

Chapter 1, in part, is a reprint of the material as it appears in "Rapid biodegradation of renewable polyurethane foams with identification of associated microorganisms and decomposition products" in Bioresource Technology 2020. Gunawan, Natasha R.; Tessman, Marissa; Schreiman, Ariel C.; Simkovsky, Ryan; Samoylov, Anton A.; Neelakantan, Nitin K.; Bemis, Troy A.; Burkart, Michael D.; Pomeroy, Robert S.; Mayfield, Stephen P. The thesis author was an investigator and third author of this material.

Chapter 2: Isolation and Characterization of Bacteria that Hydrolyze Polyurethane Foam

2.1 Serial Passaging of Environmental Inoculum

To identify organisms from compost and soil capable of utilizing the PU to grow, organisms were inoculated into M9 minimal media supplemented with nutrients (MIN, Table A1), with PU added as the sole carbon source. PU foam was frozen in dry ice and pulverized with a high-speed blender to create fine particulates and then autoclaved to ensure sterility. In 125 mL Erlenmeyer flasks, 25 mL of MIN media and 0.5 g PU particulate were prepared. 1 g of material from either compost or soil, designated as the inoculum, was added to separate flasks, along with environmental control flasks with inoculum but no PU and a control flask with MIN+PU media but no inoculum. Compost was collected from UCSD Roger's Community Gardens and soil was collected from UCSD Solis Hall. Flasks were shaken at 100 rpm at room temperature. 1 mL of the liquid in the flask was then used to inoculate a fresh MIN+PU media flask for the sub- sequent passage. Fresh flasks were inoculated weekly for 8 weeks and then bi-weekly at weeks 10 and 12 for a total of 10 passages. At the end of each passage, 1:1000 and 1:10,000 dilutions were prepared and 50 μL was plated onto lysogeny broth (LB, BioPioneer cat# CMLP-1) and potato dextrose agar (PDA, Millipore Sigma cat# P2182) media and grown at room temperature for 48 h. Individual colonies with unique morphology were picked from each plate from the 10^{th} passage. ThermoFisher Phire Plant Direct PCR Master Mix (cat# F160S) with appropriate primers for 16S (515F, 806R) and ITS1 (ITS1-F, ITS2) were used to PCR amplify each selected colony (Parada, Needham, and Fuhrman 2016; Apprill et al. 2015; Gardes and Bruns 1993; White et al. 1990). The samples were sent to Eton Biosciences for Sanger sequencing (Dovichi 1997).

Table 1: List of isolated bacterial strains after ten passages in MIN+PU media, based on 16S sequencing results.

Environment	Family	Genus
Compost	*Burkholderiaceae*	*Achromobacter*
	Brucellaceae	*Brucella*
	Pseudomonadaceae	*Pseudomonas*
	Rhizobiaceae	*Rhizobium*
	Xanthomonadaceae	*Stenotrophomonas*
Soil	*Flavobacteriaceae*	*Chryseobacterium*
	Oxalobacteraceae	*Herbaspirillum*
	Brucellaceae	*Ochrobactrum*
	Nocardiaceae	*Rhodococcus*
	Xanthomonadaceae	*Stenotrophomonas*

In total, ten bacterial strains were isolated after the final passage, five from the compost inoculum and five from the soil inoculum (Table 1). Many of these bacteria come from genera which are known to biodegrade plastic materials (Gan and Zhang 2019). Both Rhodococcus and Pseudomonas bacteria have been found previously to biodegrade PU materials, so the Pseudomonas isolate from compost (Ps) and the Rhodococcus isolate (Rh) from soil were selected for further experiments (Gu and Mitchell 2004; Peng et al. 2014). In addition, both of these genera are known to have large and varied genomes which incorporate many metabolic pathways, so they are more likely to have enzymes with urethanase activity (McLeod et al. 2006; Espinosa et al. 2020). Frozen glycerol stocks of all isolates were prepared by growing organisms in LB media for

48 hr at room temperature and shaking at 100 rpm, then diluting 1:1 with a sterile 50% v/v solution of glycerol and LB media and stored at -80℃ (Hubálek 2003).

2.2 Growth Rate Measurements

A sterile loop was used to inoculate 25 mL solutions of MIN+PU with either Pu or Rh and 100 µL of media was sampled every day for the first 8 days, and then at 30 days and 45 days. All samples were grown at room temperature and shaken at 100 rpm. Samples were measured using the Tecan infinite M200 Pro UV-vis spectrometer in a Thermo Scientific™ Nunc™ Edge™ 96-Well, Flat-Bottom Microplate (cat# 267427) plate for their optical density at 600 nm (OD600). MIN media was also measured to determine the baseline OD600 (Domańska et al. 2019). Fold change was determined using the following equation: $\Delta Fold_{day\,x} = \frac{OD600_{day\,x} - OD600_{MIN}}{OD600_{day\,0} - OD600_{MIN}}$ and plotted on a logarithmic scale (Figure 3).

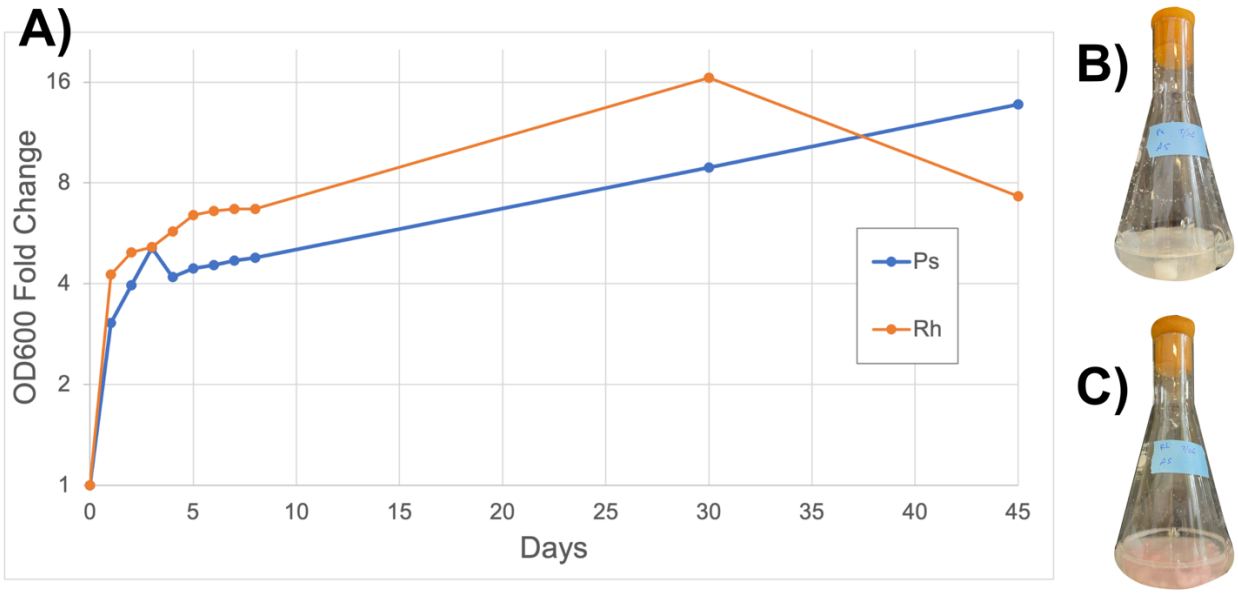

Figure 3: A) Logarithmic plot of the fold-change in OD600 from the initial value for both Ps (blue) and Rh (orange) over 45 days. B) Image of Ps grown for 4 days in MIN+PU media. C) Image of Rh grown for 4 days in MIN+PU media.

The OD600 values clearly indicate that Ps and Rh can grow and multiply in MIN+PU media for at least one month, confirming the results from the serial passaging experiment. Interestingly, two phases of growth are visible: an early period of rapid growth for the first 3–5 days that results in approximately two doublings. Afterwards, growth slows and bacteria double another once or twice over the next two weeks. A possible explanation for this is that the PU foam undergoes partial hydrolysis when autoclaved, providing an easier carbon source for the first few days, then growth slows as bacteria must hydrolyze the PU before being able to consume the resulting monomers. For future experiments, Ps and Rh will be harvested at 4 days during the transition between these two phases of growth.

2.3 Whole Genome Sequencing of Rhodococcus and Pseudomonas Isolates

Glycerol stocks of each isolate were plated onto LB media and grown at room temperature over 96 hr for Rh or 48 hr for Ps, then colonies were picked and grown in 4 mL of LB media for 72 hr at room temperature while shaking at 120 rpm. Genomic DNA from two 2 mL aliquots of each culture were prepared using the QIAGEN Dneasy UltraClean Microbial Kit (cat# 12224) using the recommended protocol with two exceptions: cells were pelleted for 2 min instead of 30 sec and both aliquots of each colony were pooled to yield 100 µL of purified genomic DNA (Elizaquível and Aznar 2008). A ThermoFisher Scientific Qubit 2.0 Fluorometer was used to quantify DNA yields using the recommended protocol for the Qubit™ dsDNA HS Assay Kit (cat# Q32851), and the sample with the highest concentration for each strain was used for sequencing, and that cultured saved as a glycerol stock in the same procedure outlined in Section 2.1 (Mardis and McCombie 2017).

60 µL of purified genomic DNA with concentration 48.4 ng/µL (Rh) or 115 ng/µL (Ps) were shipped overnight on ice to the Microbial Genome Sequencing Center (MiGS) for sequencing

where samples were prepared for sequencing on the Illumina NextSeq 2000 platform to a read depth of 400 Mb and on the Oxford Nanopore platform to a read depth of 300 Mb (Besser et al. 2018). Quality control and adapter trimming was performed with bcl2fastq version 2.20.0.445 and porechop version 0.2.3_seqan2.1.1 for Illumina and Nanopore sequencing, respectively (bcl2fastq2 Conversion Software v2.20 2019; R. Wick 2018). Hybrid assemblies with Illumina and Nanopore reads were performed with Unicycler version 0.4.8 (R.R. Wick et al. 2017). Assembly statistics were recorded with QUAST version 5.0.2 (Gurevich et al. 2013). Each program was run with default parameters.

Assembled genomic sequences were uploaded to the Genemark.hmm prokaryotic server version 3.26 which uses a heuristic model to predict gene sequences in each genome (Besemer, Lomsadze, and Borodovsky 2001). The program was run with default parameters and Rhodococcus_erythropolis_PR4 (Rh) or Pseudomonas_putida_F1 (Ps) were used as the model species for the predictions. Next, each assembly was uploaded to the Microbial Genomes Atlas (MiGA) to be compared with the set of all complete, non-redundant NCBI prokaryotic genomes on the basis of Average Nucleotide Identity (ANI) to determine the taxonomy of each isolate (Rodriguez-R et al. 2018). The MiGA server confirmed previous sequencing results for the genus identification with p-value 0.024 for Ps and 0.22 for Rh, and further concluded that both isolates represent species not included in the database with p-value 0.0043 for Ps and 0.0025 for Rh. The 16S sequences were compared against the rRNA_typestrains/16S_ribosomal_RNA database using BLAST to identify other close relatives of each isolate (Zhang et al. 2000). MiGA also identified all the gene sequences in each assembly, with similar results to GeneMark, and found that a very high percentage of canonical essential prokaryotic genes were present in both Ps and Rh, further supporting the validity of the sequencing data.

Finally, the draft assembly was polished to produce consensus sequences for each isolate. Circlator, run with the parameters --merge_min_id 85 and --merge_breaklen 1000 and using SPAdes version 3.15.2 for the alignment step, was used to ensure that each contig was either the main circular genome or a plasmid (Hunt et al. 2015; Li 2013; Kurtz et al. 2004; Hyatt et al. 2010; Li et al. 2009; Bankevich et al. 2012). Bandage was used to visualize assembly graph files (R.R. Wick et al. 2015). Circularization failed with these parameters for Rh, although the Bandage graph suggests there is a circular chromosome for Rh (Figure A1). As a final step, medaka (Oxford Nanopore Technologies Ltd., version 1.4.3) command medaka_consensus was run with parameters -t 4 -m r941_min_high_g303 to create a polished consensus assembly.

Relevant information regarding the assembly and gene prediction steps are presented below (Table 2). Sequencing coverage was estimated for both the Illumina and Oxford Nanopore reads (Lander and Waterman 1988). These results support the conclusion that Ps is a novel bacterial species from the genus *Pseudomonas* with a single circular chromosome of length 5.5 Mb and approximately 5000 genes, and Rh is a novel bacterial species from the genus *Rhodococcus* with 4 linear contigs with total length 6.6 Mb and approximately 6000 genes. However, Rh assembly may require further tweaks to connect and circularize contigs. When compared with the GenBank database, these values suggest that both isolates have robust genomes which are larger than average in size and total number of genes for bacteria (Saladi 2018). Assembled genomes will be uploaded to GenBank once this research is completed and prepared for publication.

Table 2: Genomic assembly validation and statistics.

	Read depth	Assembly contigs	GC content	Number of genes identified by GeneMark	Closest relative by ANI	Closest relative by 16S	Percentage essential genes	Number of genes identified by MiGA	Contigs circularized by circlator
Ps	Illumina: 3.4 million read pairs (195x coverage) Nanopore: 530 thousand reads (385x coverage)	1: 5,123,415 bp 2: 387,141 bp	65%	5042	*Pseudomonas putida* (87.5% identity)	*Pseudomonas plecoglossicida* (98.7% identity)	99.1%	4948	Joined 1 and 2 and circularized. After polishing: 5,508,241 bp
Rh	Illumina: 2.6 million read pairs (115x coverage) Nanopore: 560 thousand reads (375x coverage)	1: 5,371,687 bp 2: 1,026,871 bp 3: 109,834 bp 4: 75,076 bp 5: 383 bp 6: 131 bp	62%	6167	*Rhodococcus imtechensis* (72.3% identity)	*Rhodococcus qingshengii* (100% identity)	98.1%	6045	Circularization failed. After polishing, 4 contigs: 1: 5,371,122 bp 2: 1,020,856 bp 3: 109,841 bp 4: 75,077 bp

2.4 Mass-Spectrometry Proteomics of Bacterial Isolates

While whole genome sequencing provides a great deal of information about each bacterial isolate, it does not directly explain which genes are responsible for PU degradation. There are several methods for identifying potential gene targets with the desired function, including transcriptomics, gene cluster identification, and functional annotation, but these methods typically rely on prior knowledge of similar genes in other organisms (Tyers and Mann 2003). Incorporating proteomics into the enzyme identification pipeline, due to improvements in the sensitivity and accuracy of protein mass-spectrometry in recent years, has become a feasible method of quantifying changes in protein expression due to changes in culture conditions (Schubert et al. 2017). Notably, these identifications do not require *a priori* knowledge of enzyme function and can therefore result in unexpected enzyme function. For example, a caprolactamase enzyme was recently isolated and characterized after quantitative protein mass-spectrometry analysis of a caprolactam-degrading strain of *Pseudomonas* bacteria; while previous literature had suggested a

lactamase would be responsible, authors instead identified an ATP-dependent oxoprolinase enzyme (Otzen, Palacio, and Janssen 2018).

A similar situation exists for identifying urethanase enzymes. While many urethanase enzymes have been reported from a wide variety of enzyme classes including lipases, cholesterol esterases, cutinases, proteases, amidases, and ureases, the majority have only been demonstrated to hydrolyze the ester bonds in the polyester portions of PU, instead of the urethane bonds (Magnin et al. 2021; Biffinger et al. 2015). A few studies have proven urethanase activity directly, however these have focused either on degradation of the non-PU chemical ethyl carbamate, or have used enzymes for which the amino acid sequences are not publicly available (Magnin et al. 2019; Masaki et al. 2020; Akutsu-Shigeno et al. 2006; Gunawan et al. 2020; Santerre and Labow 1997; Gamerith et al. 2016).

To determine the sequence of one possible urethanase enzyme, cholesterol esterase from *Pseudomonas sp.* produced by MP Biomedicals (cat# 0210543982), which is shown in Chapter 4.4 (Gunawan 2020) to hydrolyze urethane bonds, was boiled in Tris/Glycine buffer (Bio-Rad, cat# 1610771) and run on a Mini-PROTEAN® TGX Stain-Free™ Precast Gel (Bio-Rad, cat# 4568033) at 100V for 1 hr. After Coomassie staining (Thermo Scientific™, SimplyBlue™ SafeStain, cat# LC6060) and comparison with AccuRuler RGB PLUS Prestained Protein Ladders (cat# G02102), two bands of approximately 30 kDa and 60 kDa (Figure 4) were excised, trypsinized, and sequenced with Reverse Phase C18 Resin Liquid Chromatography Mass-Spectrometry by the UCSD Biomolecular and Proteomics Mass Spectrometry Facility (BPMSF) according to their protocols (https://bpmsf.ucsd.edu/training-protocols/protocols.html). Two enzymes from *Pseudomonas aeruginosa*, a 311-amino-acid lipase (WP_003119862.1) and a 536-amino-acid aminopeptidase (AAG06327.1) were identified as having the best alignment with the

protein fragments (Figure 4). The lipase has 46% amino-acid sequence identity with a gene labeled Ps_535 from the GeneMark annotation of the Ps draft assembly.

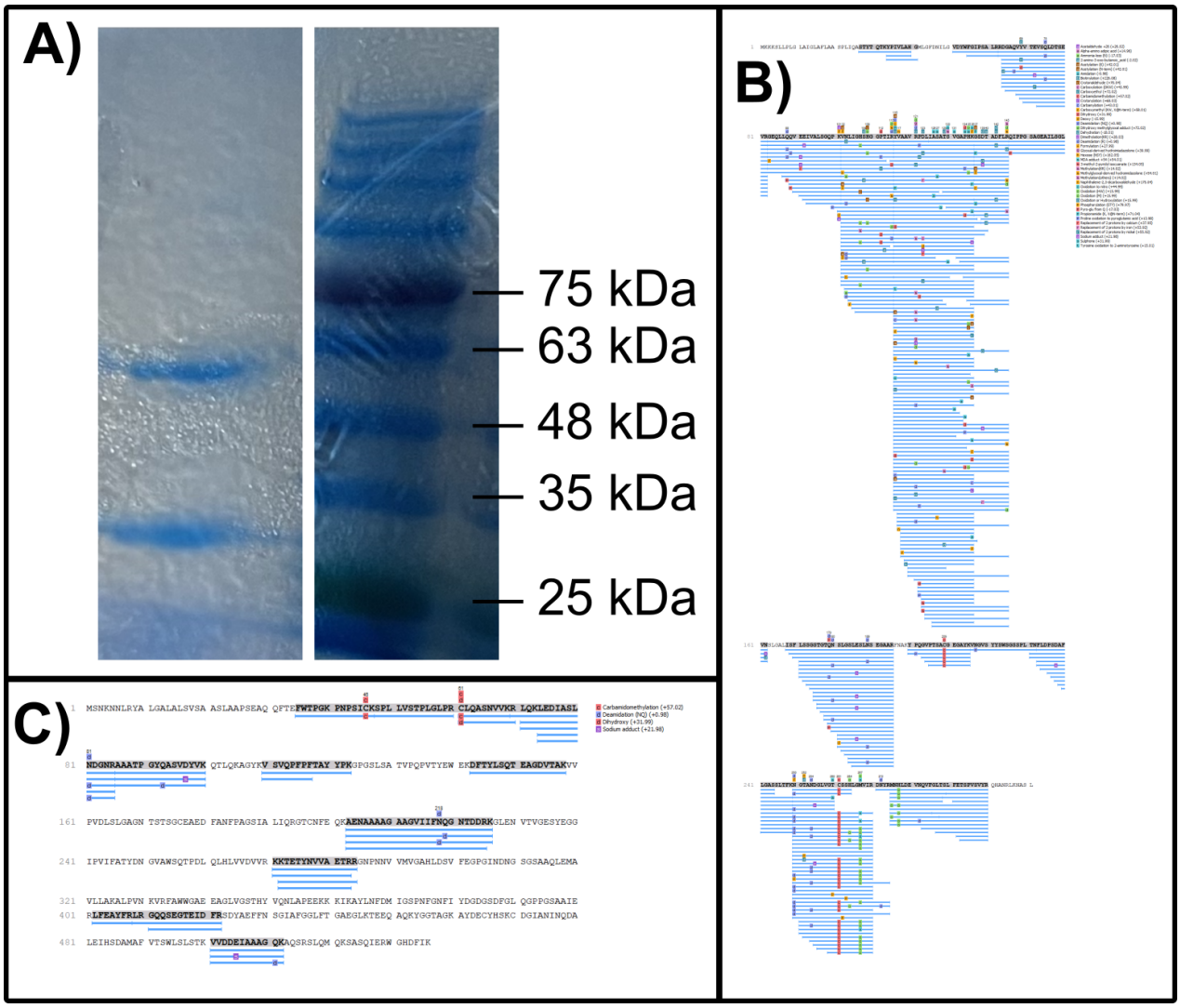

Figure 4: A) Polyacrylamide gel image of the cholesterol esterase and the ladder, with an empty lane in the middle cropped out. B) Alignment of protein fragments from the ~30 kDa band with the *Pseudomonas aeruginosa* lipase. C) Alignment of protein fragments from the ~60 kDa band with the *Pseudomonas aeruginosa* aminopeptidase.

Given that these data only provide two potential urethanase sequences, neither of which has a high degree of similarity to the genes in the Ps isolate, and there are no available urethanase sequences from a *Rhodococcus*, it is not currently possible to easily identify potential urethanase

genes solely from the genomic assemblies of these two isolates, necessitating the use of proteomics.

Isolates were grown in 10 mL cultures of MIN media supplemented with either 0.4% w/v dextrose or 2.0% w/v PU foam prepared as described in Section 2.1. All samples were grown at room temperature and shaken at 100 rpm for 96 hr, except for the Pseudomonas with dextrose condition, which was only grown for 48 hr to avoid overgrowing the culture. Cultures with foam were filtered through cheesecloth to remove residual plastic debris. Each culture was centrifuged for 5 min at 10,000 g and 4°C to pellet cells, and supernatant was transferred to a new tube. Total wet cell pellet mass was measured for each sample: 3.2 mg for Ps in MIN+PU, 35.2 mg for Ps in MIN+dextrose, 15.7 mg for Rh in MIN+PU, and 19.2 mg for Rh in MIN+dextrose. The cell pellet was resuspended in 10 mL of MIN media and lysed by sonication (Fisher Scientific Sonic Dismembrator Model 500, amplitude 29% for 1 min) then all eight samples were lyophilized overnight.

Lyophilized samples were provided to BPMSF where they were prepared with the Thermo Scientific™ Tandem Mass Tag™ protocol "User Guide: TMT10plex Mass Tag Labeling Kits and Reagents" – protein extracted, reduced, alkylated, digested overnight, labeled with reagent, mixed, then fractionated – and processed on an Orbitrap Fusion Lumos Tribrid Mass Spectrometer. Raw data was first processed with Thermo Scientific™ Proteome Discoverer™ 2.1. Then the GeneMark gene lists for each isolate were used as the reference for data processing with Bioinformatics Solutions Inc. PEAKS Studio Xpro to search for protein sequences matching identified peptides. Proteins which were expressed 3-fold more with significance greater than 20 and length longer than 100 amino-acids in either the cell pellet or the supernatant were designated as potential expression targets: 24 total for Rh and 126 total for Ps.

Chapter 2, in part, is a reprint of the material as it appears in "Rapid biodegradation of renewable polyurethane foams with identification of associated microorganisms and decomposition products" in Bioresource Technology 2020. Gunawan, Natasha R.; Tessman, Marissa; Schreiman, Ariel C.; Simkovsky, Ryan; Samoylov, Anton A.; Neelakantan, Nitin K.; Bemis, Troy A.; Burkart, Michael D.; Pomeroy, Robert S.; Mayfield, Stephen P. The thesis author was an investigator and third author of this material.

Chapter 3: Urethanase-Activity Prediction and Enzyme Expression

3.1 Selection of Enzyme Targets

Each protein of interest identified in Chapter 2 was searched using BLASTP version 2.12.0+ with the refseq_protein database to identify likely function based on homology to known enzymes (S. F. Altschul et al. 1997; Stephen F. Altschul et al. 2005). Among these, 9 likely hydrolase enzymes from Ps and 4 from Rh were identified. The 4 hydrolase genes with highest expression from Ps and the 3 hydrolase genes from Rh with highest expression were selected to be expressed in *E. coli*. In addition to these 7 genes, two more were selected from Ps which did not appear in the proteomics data. The first is the gene Ps_535, which has homology to a known urethanase, as described in Section 2.4. The second is Ps_3046, which has 74% sequence similarity with an arylesterase gene identified in the genome of a PU-degrading *Pseudomonas* isolate (Stamps et al. 2018). Finally, the PueB gene from *Pseudomonas chlororaphis* (AAF01331.1), was selected as a positive control for its known lipase activity against the aqueous PU suspension Impranil®DLN SD (Impranil), and was codon optimized and ordered through Integrated DNA Technologies Codon Optimization Tool and gBlocks HiFi Gene Fragments (Howard, Crother, and Vicknair 2001). These ten genes were then run through the structure and function prediction server I-TASSER as an independent verification of the likely function of each gene (Roy, Kucukural, and Zhang 2010; J. Yang et al. 2015; J. Yang and Zhang 2015). Finally, structural predictions from the I-TASSER server were used to simulate binding to methylene bisphenyl dicarbamic acid dibutyl ester (MDBC), a PU analogue, using the SPOT-ligand2 online server, which provides a binding score that enables relative comparison of the likelihood of protein–ligand interactions (Litfin, Zhou, and Yang 2017; Y. Yang, Zhan, and Zhou 2016). A summary of these results is presented below and the full amino acid sequences are in the appendix (Table 3, Table A2).

Table 3: Summary of known information for the 10 chosen enzyme expression targets. Identification method column provides the fold difference in protein expression from the dextrose and the PU media if the gene was identified in the proteomics.

Gene name	Identification method	Size (amino acids)	Most similar protein in refseq_protein database	Top two Enzyme Commission numbers predicted by I-TASSER	Top two Gene Ontology molecular functions predicted by I-TASSER	SPOT-ligand2 score for MDBC binding
Ps_2438	Proteomics: 7.7x in cell pellet 20x in supernatant	724	**TULIP family P47-like protein** (100% coverage, 85% sequence identity) ID: WP_196145277.1	**7.1.2.1** P-type H^+-exporting transporter **3.4.11.2** Membrane alanyl aminopeptidase.	**0043167** Ion binding. **0003824** Catalytic activity.	0.094
Ps_4943	Proteomics: 12.5x in cell pellet 8.5x in supernatant	152	**YbaK/EbsC family protein** (100% coverage, 95% sequence identity) ID: WP_084855408.1	**6.1.1.15** Proline–tRNA ligase. **1.1.1.37** Malate dehydrogenase.	**0043906** Ala-tRNA(Pro) hydrolase activity. **0005515** Protein binding.	0.248
Ps_4451	Proteomics: 2.5x in cell pellet 3.1x in supernatant	629	**Autotransporter domain-containing SGNH/GDSL hydrolase family protein** (100% coverage, 85% sequence identity) ID: WP_186552664.1	**3.1.1.1** Carboxylesterase. **2.3.1.54** Formate C-acetyltransferase.	**0052689** Carboxylic ester hydrolase activity. **0016298** Lipase activity.	0.132
Ps_1958	Proteomics: 3.6x in cell pellet 2.3x in supernatant	598	**Trypsin-like peptidase domain-containing protein** (100% coverage, 96% sequence identity) ID: WP_174215672.1	**2.7.7.48** RNA-directed RNA polymerase. **3.4.21.98** Hepacivirin. (peptidase family S29)	**0005524** ATP binding. **0003723** RNA binding.	0.252
Ps_3046	Homology to arylesterase from PU-degrading *Pseudomonas*	201	**Arylesterase** (100% coverage, 92% sequence identity) ID: WP_012313662.1	**3.1.1.5** Lysophospholipase. **3.1.1.72** Acetylxylan esterase.	**0047617** Acyl-CoA hydrolase activity. **0004622** Lysophospholipase activity.	0.150
Ps_535	Homology to lipase identified in known urethanase	296	**Triacylglycerol lipase** (100% coverage, 93% sequence identity) ID: WP_153785560.1	**3.1.1.3** Triacylglycerol lipase. **1.11.1.10** Chloride peroxidase.	**0004806** Triglyceride lipase activity. **0046872** Metal ion binding.	0.213
Rh_477	Proteomics: 5.3x in cell pellet 5.7x in supernatant	309	**Glycoside hydrolase family 43 protein** (100% coverage, 100% sequence identity) ID: WP_029254239.1	**3.2.1.26** Beta-fructofuranosidase. **3.2.1.80** Fructan beta-fructosidase.	**0004553** Hydrolase activity, hydrolyzing O-glycosyl compounds. **0016758** Hexosyltransferase activity.	0.144
Rh_2293	Proteomics: 5.9x in cell pellet 4.6x in supernatant	435	**Serine hydrolase** (100% coverage, 100% sequence identity) ID: WP_153211463.1	**3.1.1.1** Carboxylesterase. **3.4.16.4** Serine-type D-Ala-D-Ala carboxypeptidase.	**0008800** Beta-lactamase activity. **0005515** Protein binding.	0.310
Rh_4826	Proteomics: 5.9x in cell pellet 11.3x in supernatant	191	**C40 family peptidase** (92% coverage, 100% sequence identity) ID: WP_029255974.1	**2.3.1.164** Isopenicillin-N N-acyltransferase. **3.6.4.13** RNA helicase.	**0016880** Acid-ammonia (or amide) ligase activity. **0016811** Hydrolase activity, acting on carbon-nitrogen (but not peptide) bonds, in linear amides.	0.086
PueB	Impranil-hydrolyzing enzyme from *Pseudomonas chlororaphis*	567	Known protein, ID: AAF01331.1	**3.1.1.3** Triacylglycerol lipase. **2.4.2.29** tRNA-guanosine(34) preQ(1) transglycosylase.	**0005509** Calcium ion binding. **0004806** Triglyceride lipase activity.	0.124

The functional prediction and ligand-binding results were then used to create a priority list of the enzymes. Because of the chemical similarity between amide and peptide bonds and urethane bonds, priority was given to predicted amidase and protease enzymes: Ps_1958, Rh_2293, and Rh_4826; in addition, priority was given to enzymes predicted to bind better to MDBC: Rh_2293, Ps_1958, and Ps_4943. Interestingly, although PueB is predicted to bind well to PU structures, a number of the genes identified have higher predicted affinity for MDBC (do Canto, Thompson, and Netz 2019). Given timing limitations, it was decided to first express just one of these enzymes. Rh_4826 was chosen because of its functional prediction, small size, and high expression in the Rh PU supernatant in the proteomics experiment.

3.2 Cloning of Rh_4826 into Escherichia coli

The pET vector system was chosen for expression of recombinant Rh_4826 in *E. coli*. The pET vectors are based on the earlier pBR322 vector, which was designed as a small molecular weight plasmid of medium copy number with a variety of advantageous restriction digest sites for cloning (Bolivar et al. 1977). The pET28a vector improves on this model by incorporating the T7 bacteriophage polymerase system to drive expression of the transgene, along with a multiple cloning site, a *lac* operon system for repression of transgene expression until induced by isopropyl-β-d-thiogalactopyranoside (IPTG), and a hexahistidine tag (6xHis) at both the C- and N-termini (Dubendorff and Studier 1991; Shilling et al. 2020). While the pET28a vector is not the most optimized for high transgene expression, it is very popular because of the simple 6xHis purification and Western blotting and ease of induction (Shilling et al. 2020). For expressing Rh_4826, an altered pET28a vector which had been previously used for an unpublished study, was used as the template to create the pET_Rh_4826 plasmid (Figure 5). This vector uses the Rh_4826 start codon to initiate translation and includes a Glycine-Serine-Serine linker at the C-terminus which connects

to a 6xHis tag followed by the stop codon. Vector design was performed using SnapGene Viewer Version 5.0.7 (SnapGene software from Insightful Science; available at snapgene.com) and primer design was done with the aid of the New England Biolabs (NEB) Tm Calculator, version 1.13.0 (https://tmcalculator.neb.com/).

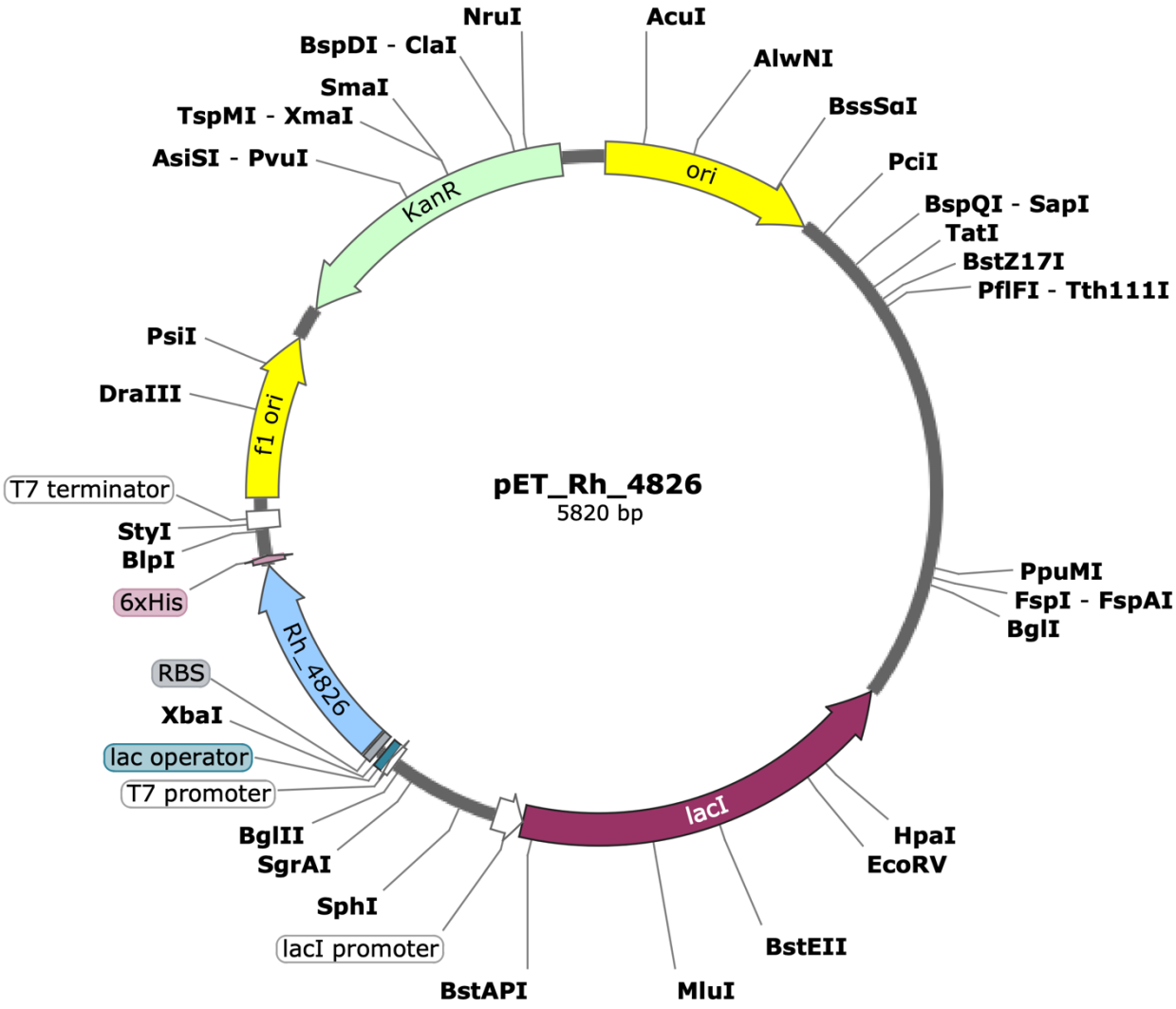

Figure 5: pET_Rh_4826 plasmid design visualization showing Rh_4826 inserted into the pET backbone along with the 6xHis tag and other notable features.

To assemble pET_Rh_4826 (Figure 5), purified genomic DNA from Rh was used as a template for a PCR reaction using Thermo Scientific™ DreamTaq 2x Master Mix (cat# K1071) and loaded with Thermo Scientific™ TriTrack loading dye (cat# R1161) onto a 1.5% agarose gel

with Invitrogen™ SYBR Safe stain added (cat# S33102) and run for 30 min at 100 V. Thermo Scientific™ GeneRuler 1 kb Plus DNA Ladder (cat# SM1331) was loaded on one lane to identify the approximate size of DNA bands. The band at the expected size was cut out and DNA was purified using the Promega Wizard SV Gel and PCR Clean-Up kit (cat# A9281) and then sent to Eton Biosciences for Sanger sequencing to confirm sequence identity, aligned to Rh_4826 using MAFFT, and visualized on Benchling (Dovichi 1997; Katoh and Standley 2013). Next, overlap sequences were added to the gene with a second PCR following the same steps. 10 ng of pET DNA from the previous study was used as the template for a PCR reaction with NEB Q5® Hot Start High-Fidelity 2X Master Mix (cat# M0494S). Then, DpnI restriction enzyme from NEB (cat# R0176S) was added to the PCR product at a dilution of 1:50 and incubated for 30 min at 37°C. 150 ul of PCR product was run on a 0.8% agarose gel for 50 min (Figure 6). Linearized plasmid bands were cut out and purified using the same Promega gel cleanup kit. All primers and PCR conditions can be found in the Appendix (Table A3).

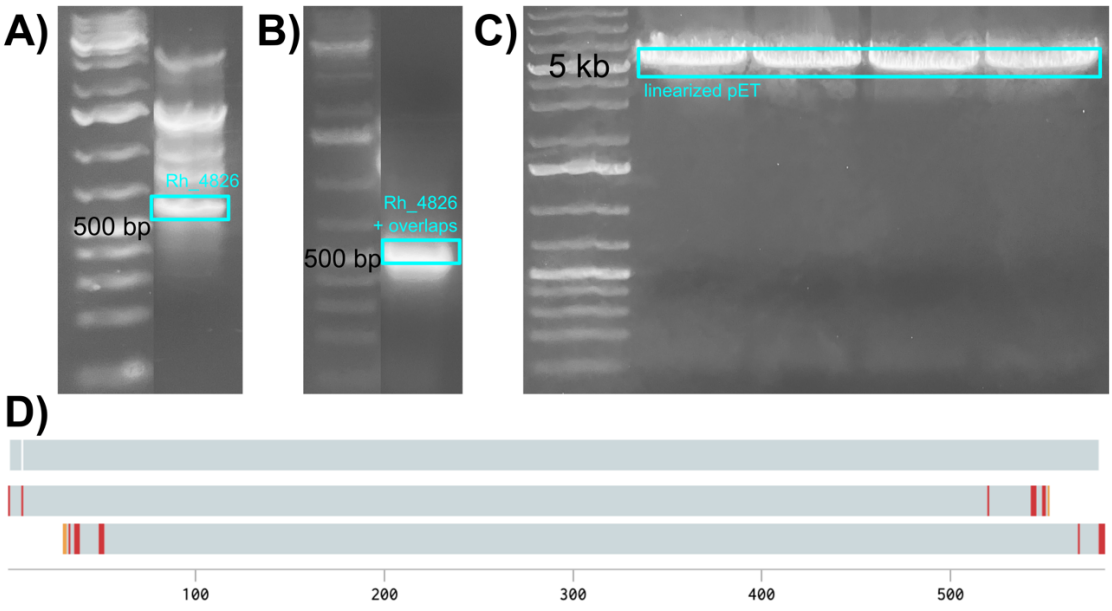

Figure 6: A) Gel image from Rh_4826 amplification, expected size 576 bp. B) Gel image from Rh_4826 overlap addition, expected size 615 bp. C) Gel image from pET linearization, expected size 5240 bp. D) Alignment of Rh_4826 sequencing results verifying correct amplification.

Plasmid assembly was performed using the NEBuilder® HiFi DNA Assembly Cloning Kit protocol (cat# E5520S) with 0.03 pmol of Rh_4826 insert and 0.015 pmol of linearized vector, based on concentrations measured by Qubit in the same method described in Section 2.3. The reaction was incubated for 15 minutes at 50°C then placed on ice and transformed into chemically-competent DH5-α *E. coli* using the NEB protocol. A positive control with the original vector and a negative control with no added plasmid were also transformed in the same manner. All three transformants were plated onto LB agar plates with 50 ug/mL kanamycin (LB+Kan) and allowed to grow at 37°C for 16 hrs. No colonies were observed on the negative control plate (Figure 7).

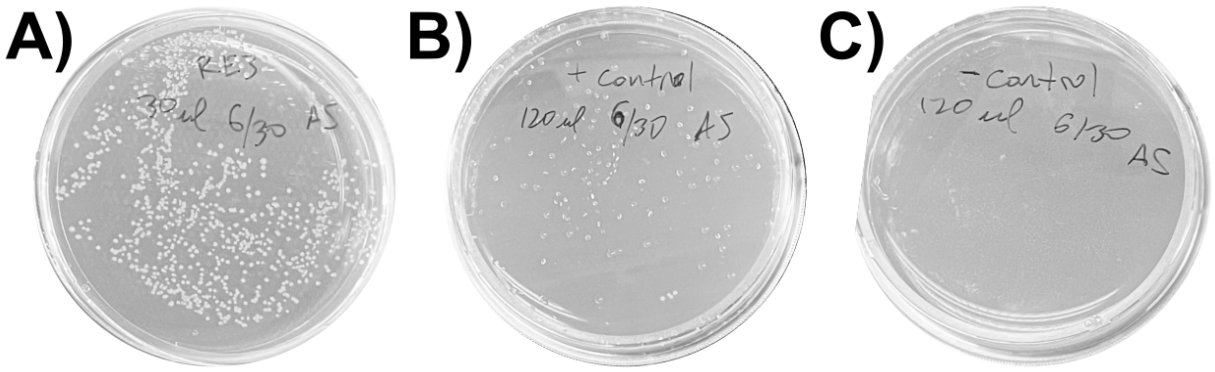

Figure 7: A) DH5-α *E. coli* transformed with pET_Rh_4826 and plated on LB+Kan. B) DH5-α *E. coli* transformed with pET vector from the previous project and plated on LB+Kan. C) Untransformed DH5-α *E. coli* plated on LB+Kan.

Two colonies were picked from the Rh_4826 transformant plate and grown in 2 mL of liquid LB+Kan media and grown at 37°C for 16 hrs while shaking at 300 rpm to make glycerol stocks in the same procedure described in Chapter 2. Frozen glycerol stocks were streaked onto fresh LB+Kan agar plates using sterile inoculating loops and grown at 37°C for 13 hrs, then one colony from each plate was used to inoculate 2 mL liquid LB+Kan cultures and grown at 37°C for 6 hrs then diluted 1:5000 into 60 mL liquid LB+Kan and shaken in a 250 mL baffled flask at 37°C for 14 hrs. Each of the two 60 mL cultures were then aliquoted into two 25 mL volumes and cells

were pelleted by centrifugation at 6000 g for 15 min at 4°C then frozen at -20°C. Each pellet was processed with the QIAGEN QIAfilter Plasmid Midi Kit (cat# 12243) to purify plasmid DNA and then the two aliquots from each original colony were pooled together and resuspended in a total of 40 uL of NEB Monarch DNA Elution buffer (cat# T1016L). Each sample was quantitated by Qubit in the same method described in Section 2.3 and the purity was verified with the Thermo Scientific™ Nanodrop Lite Spectrophotometer. The A260/A280 ratio was above 1.8 for both samples and concentrations were 397.2 ng/µL and 83.2 ng/µL, respectively. Sequences were verified via Sanger sequencing from Eton Biosciences with 80 ng/µL of plasmid DNA using the T7 Promoter and T7 Terminator primers (Table A3).

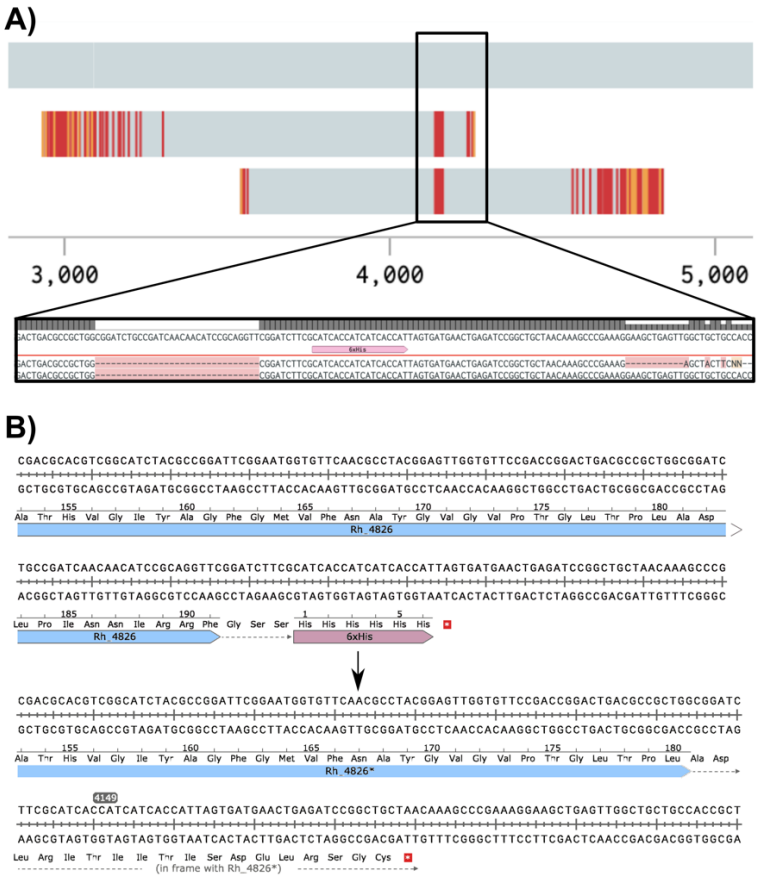

Figure 8: A) Alignment of Rh_4286 and the sequencing results for the transformed pET_Rh_4286 plasmid showing a deletion upstream of the 6xHis tag. B) Comparison of the C-terminus from the correct Rh_4286 and the mutated version, Rh_4286*, showing the amino acid changes caused by the frame shift.

Sequencing revealed that a minor deletion was present in the Rh_4286 gene (Figure 8), likely due to homology with the overlap primer used, resulting in a frame shift at the C-terminus before the 6xHis tag and changing the total length from 200 amino acids to 198 amino acids. Typically, NEB Q5® Site-Directed Mutagenesis Kit (cat# E0554S) would be used to fix this error, but due to time constraints, the mutated gene was expressed as a proof-of-concept. The plasmid containing this mutated form of Rh_4286, designated pET_Rh_4286*, was transformed into chemically-competent BL21(DE3) *E. coli* from NEB (cat# C2527H) using the standard protocol (Figure 9).

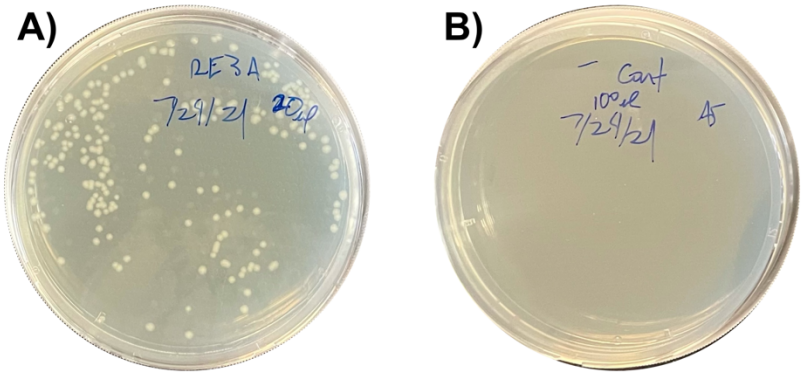

Figure 9: A) BL21(DE3) *E. coli* transformed with pET_Rh_4826* and plated on LB+Kan. B) Untransformed BL21(DE3) *E. coli* plated on LB+Kan.

*3.3 Induction of Rh_4826**

Two colonies of transformed BL21(DE3) *E. coli* containing pET_Rh_4826* were inoculated into 5 mL liquid LB+Kan cultures and grown for 10 hrs at 37°C shaking at 300 rpm, and then 0.5 mL was used to make glycerol stocks using the procedure described in Section 2.1. The remaining 4.5 mL of each culture was added to 50 mL liquid LB+Kan media in 250 mL baffled flasks. These cultures were incubated for another 1 hr at 37°C shaking at 300 rpm, then IPTG was added to a final concentration of 1.0 mM and the flasks were transferred to a 30°C shaking water bath at 300 rpm. 15 mL samples were taken from each culture at 0 hr, 3 hr, and 6 hr

after induction and immediately pelleted by centrifugation at 6000 g for 10 min at 4°C then frozen at -20°C. Pellets were later thawed and resuspended in 1000 µL of Phosphate-Buffered Saline (PBS, Table A1) media then lysed by sonication (Fisher Scientific Sonic Dismembrator Model 500, amplitude 21% for 10 sec, pause 10 sec, then amplitude 21% for 10 sec). Lysate was then clarified by filtration through a Minisart SRP 4 0.2 µm filter (cat# 17844). 30 µL of this solution was then run on a polyacrylamide gel and Coomassie stained according to the protocol described in Section 2.4 (Figure 10). In the induced samples a faint band at the expected size of 19.8 kDa is present that is not seen in the uninduced samples which indicates successful, if weak, expression of Rh_4826*.

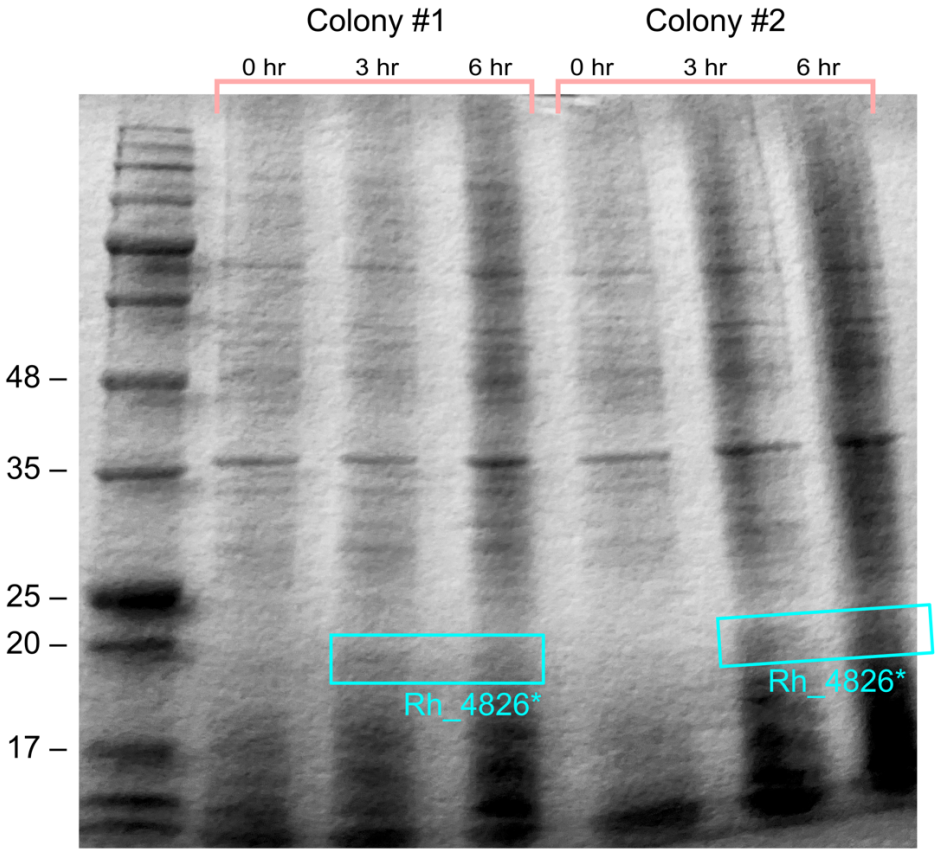

Figure 10: Coomassie-stained polyacrylamide gel of induced *E. coli* lysate. From left to right, the samples are: protein ladder, culture #1 at 0 hr, culture #1 at 3 hr, culture #1 at 6 hr, culture #2 at 0 hr, culture #2 at 3 hr, and culture #2 at 6 hr.

Chapter 4: Urethanase Activity Assays

4.1 Impranil Assay

Impranil is a colloidal PU suspension that has become the standard analytical method in PU biodegradation research and has been used frequently since its first published use in 1984. It has many advantages over other PU substrates, primarily due to its commercial availability, water-solubility, and rapid biodegradation. It is stable to hydrolysis under a variety of pH and temperature conditions and has low cytotoxicity. Analytically, it is useful because it changes from opaque to clear when hydrolyzed. However, there are many drawbacks to this assay method as well: clearing can happen from esterase activity and does not imply urethane bond hydrolysis and it is not possible to identify hydrolysis products directly because the structure for Impranil is proprietary. This has lead to ambiguity in the literature, with many microorganisms and enzymes labeled as urethanases despite the lack of direct proof of urethane hydrolysis (Biffinger et al. 2015). However, despite these flaws, Impranil is still a quick and established assay method as an initial screening step before using more involved methods to prove urethanase activity (Magnin et al. 2019). Here, Impranil is used to compare lysates from Ps and Rh grown in MIN+PU with lysate from induced BL21(DE3) *E. coli* containing the pET_Rh_4826* plasmid described in Section 3.2. Since Rh_4826* lacks the 6xHis tag which was intended to provide easy purification, an Impranil assay with crude cell lysate is an effective proof-of-concept.

To get Ps and Rh lysate, 50 mL of MIN+PU media in 250 mL baffled flasks was inoculated from glycerol stocks of Ps and Rh and then incubated for 96 hr at room temperature and shaking at 120 rpm. PU was then separated from the cell solution with cheesecloth and cells were pelleted by centrifugation at 6000 g for 15 min at 4°C. Supernatant was separated into a new tube. Pellets were resuspended in 1000 µL of Phosphate-Buffered Saline (PBS, Table A1) media then lysed by

sonication (Fisher Scientific Sonic Dismembrator Model 500, amplitude 21% for 10 sec, pause 10 sec, then amplitude 21% for 10 sec). Lysate was then clarified by filtration through a Minisart SRP 4 0.2 µm filter (cat# 17844). 15 mL of supernatant were concentrated by 3 successive loadings onto a GE Vivaspin 6 filter column with a 5 kDa cutoff (cat# 28-9322-94). Each loading was centrifuged at 6000 g for 10 min and the flow-through was discarded. Concentrated supernatant was then washed twice with 6 mL PBS, then the column retentate was removed and PBS was added to bring the final volume of 500 µL, for an effective 30x increase in concentration from the original sample.

100 µL of lysate from Ps, Rh, 6 hr-induced pET_Rh_4826* *E. coli*, uninduced pET_Rh_4826* *E. coli*, and PBS were each added in triplicate to a Thermo Scientific™ Nunc™ Edge™ 96-Well, Non-Treated, Flat-Bottom Microplate (cat# 267427). 100 µL of Impranil was added to each sample (cat# 47822612). All samples were incubated at 30°C and the OD600 was measured every 3 hr for 24 hr by a Tecan infinite M200 Pro UV-vis spectrometer and values were plotted to compare rates of Impranil hydrolysis (Figure 11). This method encountered some difficulty because of high standard deviations and variance between lysates of different samples, nevertheless it showed some promise for Ps and Rh lysates, and one of the pET_Rh_4826* induced colonies. The method would likely be more effective by using a smaller initial concentration of Impranil, measuring over 48 hr, and using greater sample sizes to reduce variance.

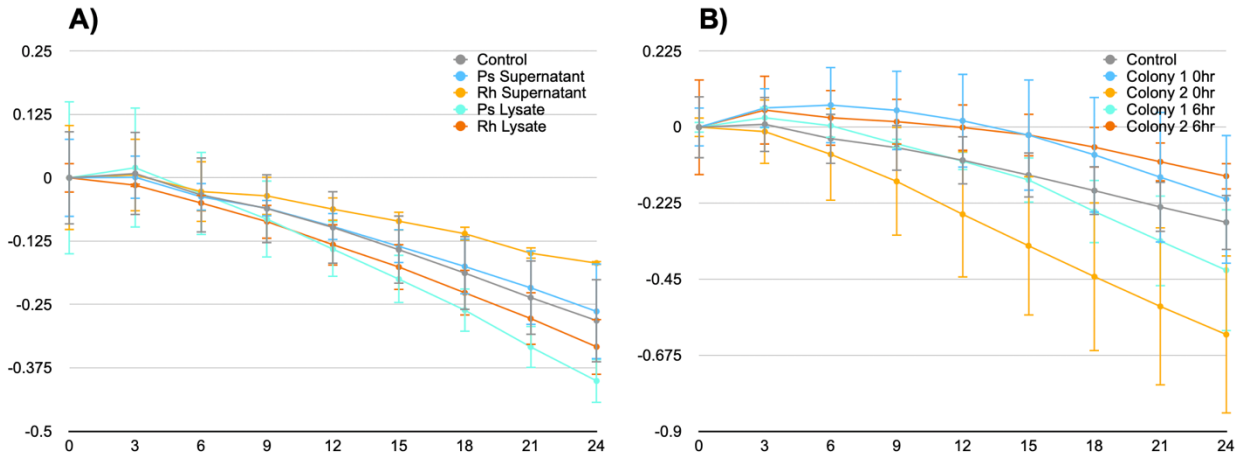

Figure 11: A) Impranil assay for lysate and supernatant from Ps and Rh, compared to control. B) Impranil assay for lysate of induced vs uninduced Rh_4826* *E. coli*, compared to control. Change in OD600 is plotted over 24 hr.

4.2 Urethanase Assay

To date, very few urethanase assays have been reported. Previous research on PU-hydrolyzing enzymes focuses on esterase activity or more directly on activity against PU, most commonly Impranil (Biffinger et al. 2015). These techniques do not actually prove hydrolysis of the urethane bond, which is unique to PU, and instead focus on the more easily hydrolyzed ester bonds in the PU material. An ethyl carbamate assay has been reported by coupling production of ammonia with the enzyme-catalyzed reaction of α-ketoglutarate into glutamate, which oxidizes the cofactor β-nicotinamide adenine dinucleotide (NADH), resulting in a change in absorbance at 340 nm (Lu, Zhou, and Tian 2015). This is a useful assay for testing hydrolysis of linear, soluble PU materials, but is not effective at mimicking aromatic isocyanate–based PU foams. More recently, an aromatic isocyanate–based assay was developed by reacting p-toluenesulfonyl isocyanate with butanol and measuring the concentration of p-toluenesulfonamide by HPLC (Magnin et al. 2019). The drawback of this assay is that it still requires a chromatography detection step, limiting throughput. However, neither of these

assays is analogous to methylene diphenyl diisocyanate (MDI) PU foam – the type used throughout this work – nor are they compatible with UV-vis spectroscopy. Therefore, development and validation of a novel spectrophotometric assay for determining urethanase activity was considered a priority before attempting to identify novel urethanase enzymes from the two bacterial isolates analyzed here.

MDBC, the product from reacting MDI and n-butanol, was chosen as the substrate of choice for this assay because it had been previously tested as a substrate for a different urethanase assay (Akutsu-Shigeno et al. 2006). During enzyme-catalyzed urethane hydrolysis, MDBC loses two n-butanol molecules and two molecules of carbon dioxide to become 4,4'-Methylenedianiline (MDA), which contains two primary amines (Doddamani and Ninnekar 2001). Primary amines can be detected with high sensitivity using 4-phenylspiro[furan-2(3H), 1'-phthalan]-3,3'-dione (fluorescamine), which reacts with primary amines to create a fluorescent molecule (Böhlen et al. 1973). Fluorescence can be rapidly and sensitively measured using a UV-vis spectrophotometer. Assay design is visualized below (Figure 12).

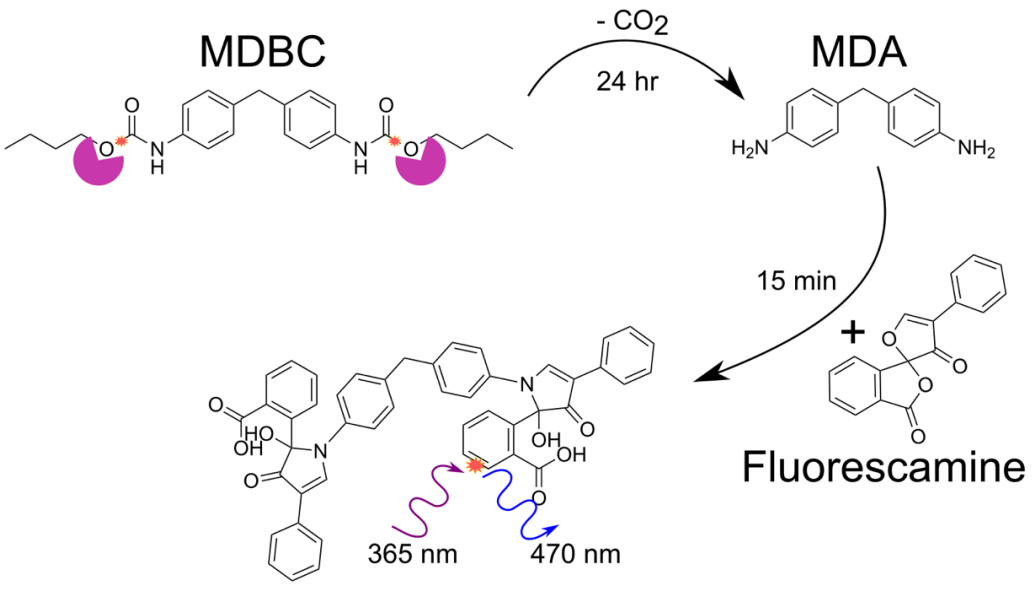

Figure 12: Diagram depicting fluorometric urethanase assay design.

Synthesis of MDBC was first attempted by dissolving 0.5 g MDI in 10 mL of n-butanol and reacting at 80°C under nitrogen gas for 2 hr. A sample was diluted and run on an Agilent Technologies Gas Chromatography–Mass Spectrometry (GCMS) system (cat# 7820A, US1374636H, 5975) with an injection volume of 1 µL, split ratio of 10:1, flow of 1.5 mL/min, a lower mass limit of 45, and an upper mass limit of 550. A pure sample of MDI was used to determine the identity of major peaks. In the reaction sample, two peaks are identified: an MDI peak and a second, smaller peak with very similar mass trace to MDI (Figure 13). The mass trace of the unknown peak contains a fragment with m/z of 324.2, which is 74.1 higher than the next major fragment of 250.1 which is the molecular weight of MDI. Butanol has a molecular weight of 74.1 g/mol, suggesting that this unknown peak is MDI reacted with a single butanol molecule. Given solubility problems of MDI in butanol and the incomplete synthesis, it was decided to make a few changes: addition of toluene to improve solubility, addition of dibutyl tin laurate catalyst, use of a condenser to decrease evaporation of solvent, and increasing the length of reaction.

0.25 g of MDI was dissolved in 5 mL of Toluene and then 5 mL of n-butanol was added. The system was sealed and nitrogen gas was introduced, then 1 µL of dibutyl tin laurate was added through a rubber septum. The reactants were then heated to 80°C and reacted for a total of 7 hr. At 2 hr and 5 hr, samples were collected and diluted in acetonitrile for analysis by High Performance–Liquid Chromatography (HPLC) on an Ultimate 3000 machine equipped with a UV-detector. At 7 hr, after allowing the reaction to cool to room temperature, a white precipitate formed. This precipitate was collected by vacuum filtration and a small sample was diluted in acetonitrile for measurement on the HPLC. In addition, a pure sample of MDA was run with the same conditions to aid in peak identification. HPLC was used instead of GCMS because of incompatibility of the dibutyl tin laurate with the GCMS column. All samples were run with an acetonitrile ramp from

10% (in MilliQ water) to 100% over 15 min and measured at 210 nm and a flow of 0.21 mL/min. Between each sample a wash of 100% acetonitrile for 10 min was performed. Reaction progress can be identified, since at 2 hr a peak likely corresponding to the partially-reacted product identified by GCMS is seen, but disappears in the later time points as a second peak appears (Figure 13). The precipitate is seen as a single peak and is presumed to be the reaction product. A total of 81.9 mg of MDBC precipitate was recovered, or about 20% of the total possible product.

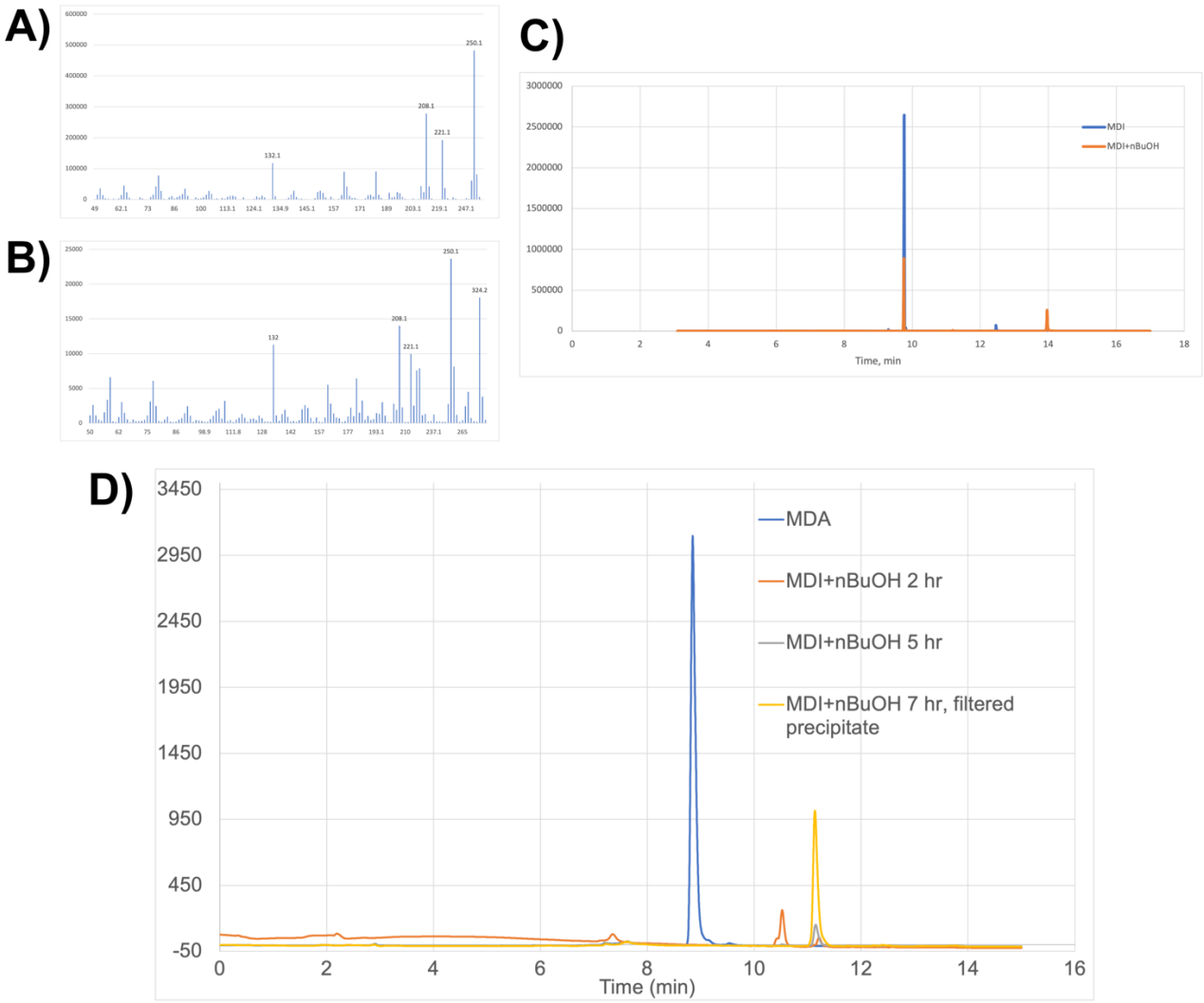

Figure 13: A) Mass trace of MDI peak on the GCMS. B) Mass trace of the unknown peak on the GCMS. C) Total ion counts for GCMS runs. D) HPLC synthesis validation by 210 nm absorption measurements.

MDBC–fluorescamine assay was validated by comparing fluorescamine fluorescence with MDA versus MDBC, since MDBC is the starting substrate and MDA is the predicted reaction product. 1 mg/mL stocks of MDBC and MDA were prepared and then diluted in PBS – 20 µL of MDBC (molecular weight 398.5 g/mol) + 980 µL PBS and 10 µL MDA (molecular weight 198.3 g/mol) + 10 µL DMSO + 980 µL PBS – for a final concentration of 50 µM MDBC or MDA and 2% v/v DMSO. 150 µL of 8 total 2-fold serial dilutions of each solution with PBS + 2% v/v DMSO were added in triplicate to a Thermo Scientific™ Nunc™ Edge™ 96-Well, Non-Treated, Flat-Bottom Microplate (cat# 267427), then 50 µL of stock 3 mg/mL fluorescamine in DMSO was added to each sample and incubated at room temperature for 15 minutes. Fluorescamine light emission at 470 nm after excitation by 365 nm light was then measured with a Tecan infinite M200 Pro UV-vis spectrometer to establish optimal measuring concentration for the assay. Strongly linear detection of MDA and low background from MDBC supports the potential effectiveness of this assay (Figure 14).

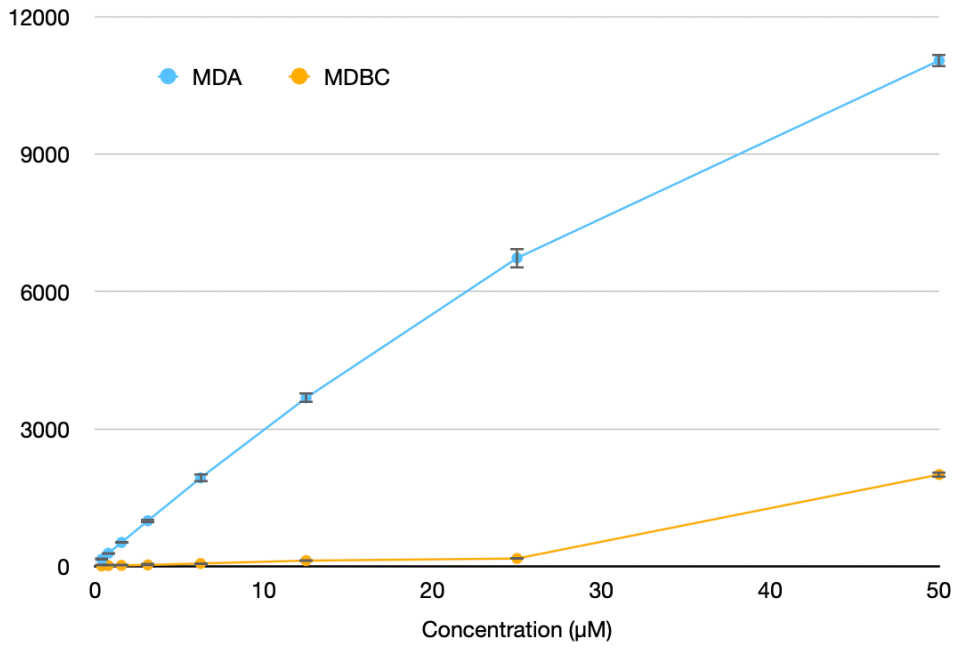

Figure 14: Calibration curve of MDBC and MDA demonstrating effective detection of MDA and low background signal from MDBC.

Determination of the amount of urethanase activity was performed by incubating MDBC with enzymes and then adding fluorescamine. Cholesterol esterase from *Pseudomonas* species (cat# C9281), lipase from *Candida rugosa* (cat# L1754), and Bovine serum albumin (BSA, cat# 9048-46-8) were diluted to a concentration of 0.1 mg/mL in PBS. 4 µL of 1 mg/mL stock MDBC in DMSO or 4 µL of DMSO was added to 196 µL of each sample (final concentration 50 µM MDBC), prepared in triplicate, and 4 µL of stock MDBC added to three 196 µL PBS control samples. Samples were incubated at 30°C for 24 hr, then diluted by 2.5 fold and 150 µL pipetted into a Thermo Scientific™ Nunc™ Edge™ 96-Well, Non-Treated, Flat-Bottom Microplate (cat# 267427). 50 µL of stock 3 mg/mL fluorescamine in DMSO was added to each sample and incubated at room temperature for 15 minutes. Fluorescamine light emission at 470 nm after excitation by 365 nm light was then measured with a Tecan infinite M200 Pro UV-vis spectrometer. PBS control demonstrates low background hydrolysis of MDBC without enzyme present. All three enzymes show some increase in fluorescence when incubated with MDBC instead of just DMSO, however the high standard deviations for lipase and esterase make it difficult to draw significant conclusions (Figure 15). Surprisingly, hydrolysis was significant in the BSA sample, and further study is needed to understand the mechanism behind this effect. Ultimately, this is a promising proof-of-concept demonstration of this assay, but follow-up tests with larger sample sizes and more time points are necessary to confirm these results.

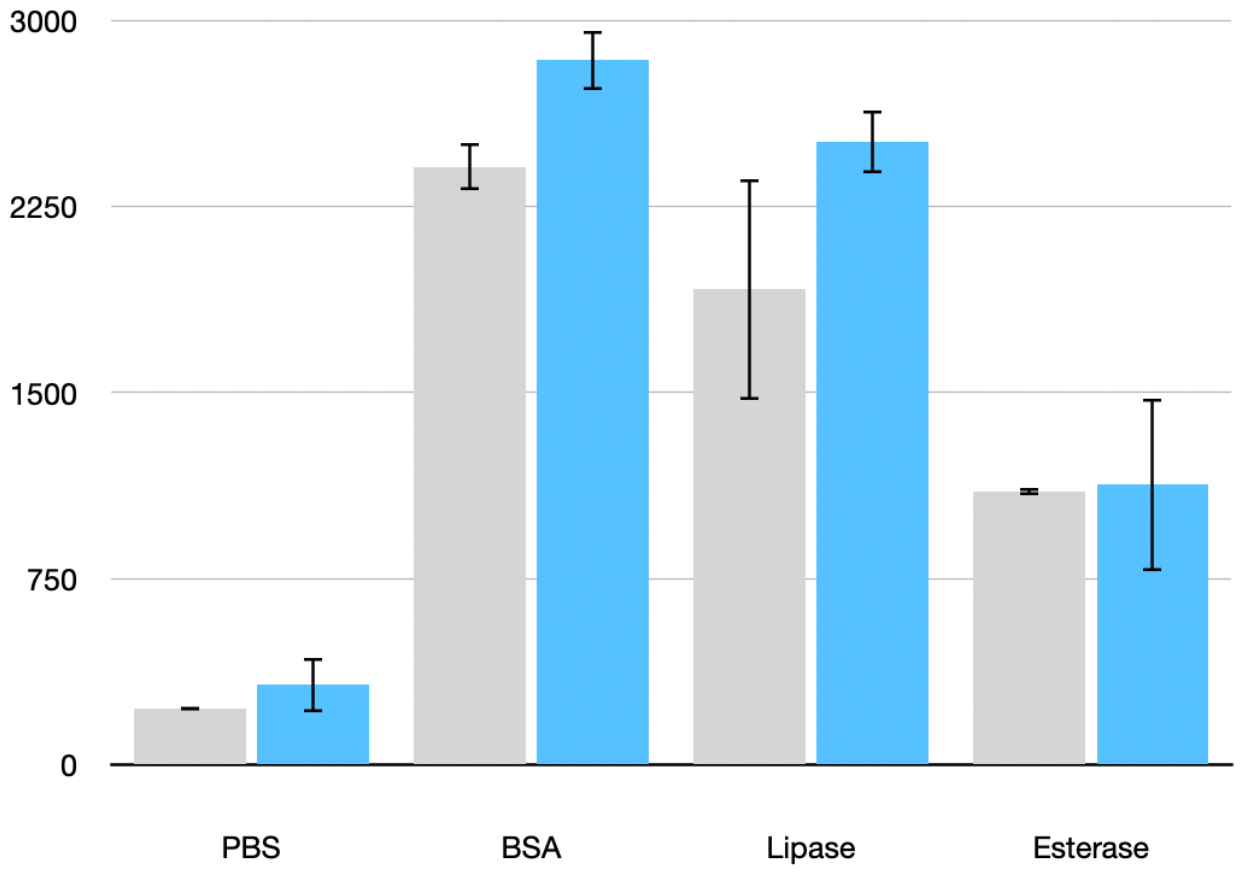

Figure 15: Fluorescence for PBS media, BSA, Lipase, and Esterase conditions, with DMSO added (grey) or MDBC added (blue).

4.3 Polyurethane Foam Assay

A mass-spectrometry-based method of directly identifying PU foam monomers produced by enzymatic degradation was developed and validated here. Critically, this demonstrates a direct chemical connection between enzyme activity and PU hydrolysis. However, because of low enzymatic activity against PU foam and the relatively (compared to fluorescence-based assays) low sensitivity, this assay can only be performed with high levels of purified enzyme. Here, only commercially-available esterases are tested, but purified recombinant protein could be tested with this system if enough enzyme – at least 2 mg – is purified for this purpose. Therefore, this assay is best used as the final validation step for a hypothesized urethanase only after performing the various simpler assays described in Sections 4.1 and 4.2.

PU foam was frozen using liquid nitrogen and crushed with a Qiagen TissueLyser (cat# 85300). Foam particulate was washed with MilliQ water to remove any soluble contaminants and then dried overnight in a desiccator. Initially, four commercial enzymes were screened for PU biodegradation activity: lipase from *Aspergillus niger* (cat# 62301), lipase from *Candida rugosa* (cat# L1754), esterase from *Bacillus subtilis* (cat# 96667) and cholesterol esterase from *Pseudomonas* sp. (cat# C9281). The microorganisms from which the enzymes were derived have been cited to have biodegradation activity (Osman et al. 2018; Gautam, Bassi, and Yanful 2007; Rowe and Howard 2002; Das and Mukherjee 2007). Bovine serum albumin (BSA) (cat# 9048-46-8) was used as a negative control. Foam was added to 1.5 mL Eppendorf tubes to a mass of 2.4 ± 0.2 mg. 1.2 mL of 400 μg/mL enzyme solution in PBS was added. All samples were prepared in triplicate. In addition, tubes containing enzymes without foam and foam without enzymes were prepared as controls. Samples were shaken for 24 h at 37 °C, then frozen immediately to prevent further enzyme activity.

For GCMS, samples were acidified and the products were extracted with ethyl acetate (EtOAc), derivatized with N-Methyl-N-trimethylsilyl trifluoroacetamide (MSTFA), and run on a GCMS similar to the method described in (Gautam, Bassi, and Yanful 2007). Chromatograms were created by subtracting the no-substrate control from an average of the triplicate sample chromatograms. 0–100 ppm standards containing diol 1, diol 2, and diacid 1, the three major chemical components of the proprietary PU foam studied here, diluted in PBS were treated to the same extraction and GCMS method. Each peak was integrated using the instrument's integration tool. The mass percent of each compound in the proprietary PU foam was known. From these values, the expected concentration of each compound at 100% PU foam degradation in parts per million and the percent degradation of the PU foam from each product was calculated by using the

mass percent of compound in the foam formulation, the mass of foam added to each sample, and the product concentration in each sample. Cholesterol esterase from *Pseudomonas* species performed the best with the highest production of diols over the course of 24 h.

For Liquid Chromatography–Mass Spectrometry (LCMS), a 50 ppm standard containing all four expected breakdown products was prepared by gentle heating in MilliQ water for several hours until complete dissolution. The standard and triplicates of the *Pseudomonas* enzyme degraded PU samples and BSA controls were filtered with a 0.22 μm syringe filter. 10 μL was injected into a Waters Acquity SQD LCMS system with a 2.1 × 150 mm 3 μm ACE C18-PFP column. The running buffers were 0.1% formic acid at pH 3.35 (A) and 100% acetonitrile (B). The run was held at 99% A at 0.2 mL/min for 7 min, then ramped to 100% B over the course of 5 min and held for 8 min before returning to the original eluent conditions over 1 min and held for 5 min to re-equilibrate. The mass spectrometer had an electrospray ionization probe set at 3.5 kV and 350°C with positive mode scan ranges from 70 to 500 m/z. Triplicate mass traces were averaged and the average traces for enzymes incubated with no foam were used for background subtraction.

The LCMS chromatograms show all four breakdown product peaks, which were not present in the BSA negative controls (Figure 16). In the GCMS chromatogram, diols 1 and 2 and diacid 1 were identified, as well as four prominent peaks at 9.8, 10.1, 11.27, and 11.47 min, which were identified by their unique mass spectra as partial degradation products: dimers and trimers of diols and diacids. To further validate the identity of the four peaks, one of the degraded samples was treated with a strong base to hydrolyze the remaining water-soluble polymer fragments. Notable in the base-hydrolyzed GCMS chromatogram was the complete disappearance of the partial PU fragment peaks and an increase of all three final product peaks, corresponding to 39 ± 3%, 43 ± 4%, and 32 ± 2% PU degradation into diol 1, diol 2, and diacid 1, respectively. These

data indicate that the cholesterol esterase degraded 38 ± 6% of the PU foam into a combination of polyol monomers and water-soluble dimers and trimers in 24 hr.

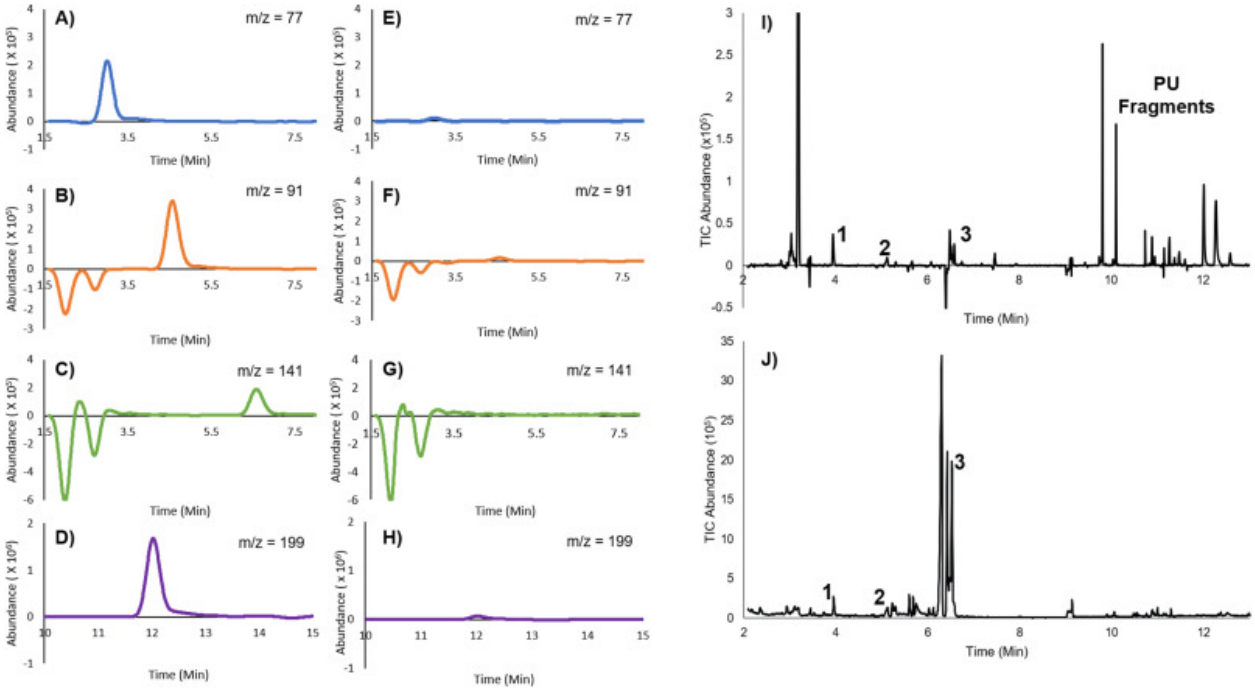

Figure 16: LCMS (left) and GCMS (right) chromatograms of enzyme-degraded PU foam. From top to bottom LCMS mass traces correspond to diol 1, diol 2, diacid 1, and MDA. **A-D)** Foam degraded with *Pseudomonas* species cholesterol esterase for 24 h. **E-F)** A negative control of foam reacted with BSA for 24 h, showing no degradation products. **I)** GCMS of *Pseudomonas* species cholesterol esterase degraded foam. 1, 2, and 3 correspond to diol 1, diol 2, and diacid 1, respectively, and PU fragments are present from 9.5 to 13 min. **J)** The same sample chemically degraded to identify the PU fragments. Note the disappearance of the peaks from 9.5 to 13 min and the increase in abundance of peaks 1, 2, and 3 to approximately 10-fold that of the original sample. Unlabelled GCMS peaks are PBS media traces.

Chapter 4, in part, is a reprint of the material as it appears in "Rapid biodegradation of renewable polyurethane foams with identification of associated microorganisms and decomposition products" in Bioresource Technology 2020. Gunawan, Natasha R.; Tessman, Marissa; Schreiman, Ariel C.; Simkovsky, Ryan; Samoylov, Anton A.; Neelakantan, Nitin K.; Bemis, Troy A.; Burkart, Michael D.; Pomeroy, Robert S.; Mayfield, Stephen P. The thesis author was an investigator and third author of this material.

Chapter 5: Discussion and Future Directions

Improvements in the recycling of plastics are necessary to move towards a true circular economy and move away from reliance on petroleum as a source of raw materials. In addition, plastic waste is a difficult environmental challenge since microplastics easily spread around the world into virtually all environments and can cause ecotoxicological and health concerns. Understanding the biodegradation of plastic is one important facet for solving this problem. Previously, Algenesis has developed a bio-based PU foam material which has been shown to biodegrade in compost and soil environments. In this thesis, this PU material was used to identify novel urethanase enzymes through a genomics and proteomics approach and one of these enzyme targets was expressed in *E. coli.* Enzymes were then tested with a combination of established and newly-developed assays. Overall, this thesis demonstrates a proof-of-concept pipeline for identifying and characterizing novel enzymes which hydrolyze PU materials.

Due to personal time limitations, not all experiments generated perfect results. The genomics and proteomics experiments went very well, but yielded more data than could be analyzed given the time constraints. The Rh genome assembly might be improved by using a different assembly tool since it failed to result in circular chromosomes or plasmids. Proteomics information could provide insight into the metabolic pathways that process PU monomers. Ideally, more than one of the identified enzymes would have been expressed, and all expressed enzymes purified using the 6xHis tag. Both the Impranil and urethanase assays would have been improved by measuring more time points and more replicates. In addition, standardizing protein concentrations by Bradford assay instead of mass might improve the consistency of enzyme assay results. Using a more sophisticated lysis protocol than just sonication might also improve protein recovery and enable better filtration to remove cell debris. All of these shortcomings, especially in

enzyme expression, are areas where next steps can be taken to improve upon these preliminary results.

In total, these data demonstrate a feasible methodology for identification and testing of new plastic-degrading enzymes. Finding and engineering these enzymes is critical for improving plastic recycling methods, which are becoming increasingly necessary as more disposable plastic is produced each year.

APPENDIX

Table A1: Media Compositions.

MIN (Gunawan et al. 2020)	
Compound	**Concentration (g/L)**
Na_2HPO_4	6.78
KH_2PO_4	3.00
NH_4Cl	1.00
NaCl	0.500
$MgSO_4•7H_2O$	0.0250
$Na_2EDTA•2H_2O$	0.0108
$FeCl_3•6H_2O$	0.00270
$FeSO_4•7H_2O$	0.00150
NaOH	0.00138
Na_2CO_3	0.00115
$CaCl_2•2H_2O$	$8.00x10^{-4}$
$MnCl_2•4H_2O$	$5.95x10^{-4}$
$ZnSO_4•7H_2O$	$3.60x10^{-4}$
$CuCl_2•2H_2O$	$1.70x10^{-4}$
$(NH_4)6Mo_7O_{24}•4H2O$	$1.75x10^{-5}$
PBS (AAT Bioquest 2021)	
Compound	**Concentration (g/L)**
NaCl	8.00
Na_2HPO_4	1.44
KH_2PO_4	0.245
KCl	0.200

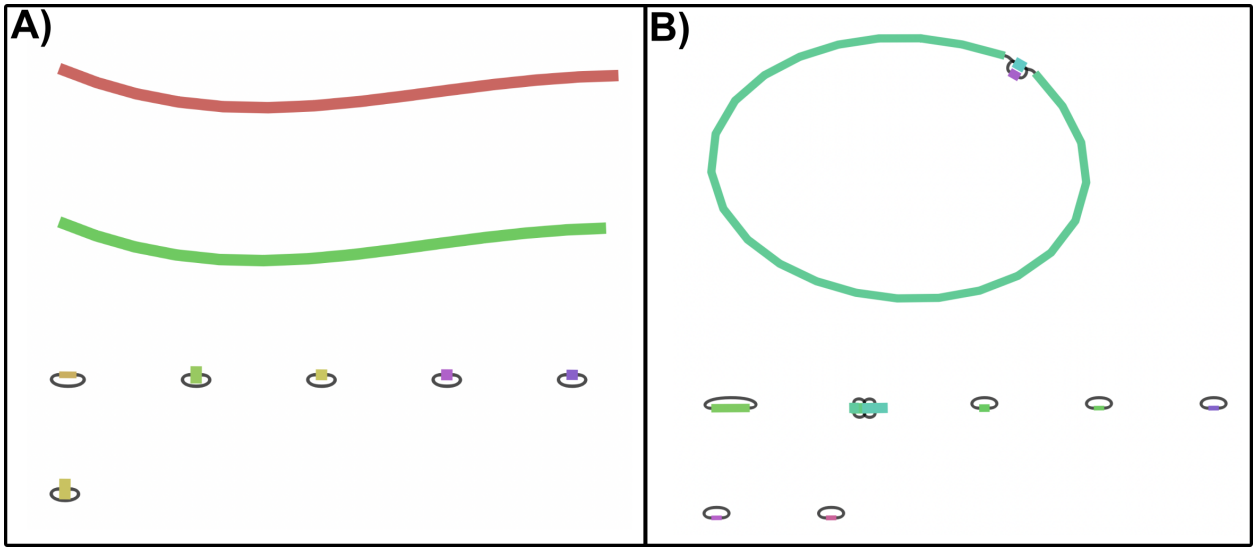

Figure A1: Visualization of sequencing contigs during circlator genome assembly polishing.

Table A2: Amino-acid sequences for all 10 proteins of interest.

Gene name	Amino-acid sequence
Ps_2438	MATPTDNTSLAPVPVSEIATRPTADTYDWDTVVALHFDTTNTALTDNW GSVDSRAKTLTQAASDDPSYQIQASLDPWQLTIGGDGKNINMSVPIASGV YQAGANSYPLDGLGMSAIIQINMDWIPDPDQKSFVINSGVAAIVADLDND IVDAALIADFAANGVTITSESKLSTVHQGAAWLIAAADNTFYYLFFSQDK DQNQFLSVYQYTKSFATQLRALSKEAGATPAVVVMNVLNPPNAGSIGN AVLPELLSEWFNSNISYFNFVFSVIDLTPQLDQSPSYTWIDPTATSYAVIDE QTMTSSVMGVLTMVQNNRPGANHQVSPNAIPTGSDANGANVGLLISGQ NFMKNMMLGGAKILFDDASDEDFSIFNDGLSIQNVNALTYGYFKMEDDP DATTADNGYSAELDSGSLPQGLVDAFKHSDGEGGYYYNPDLRGDTVKV NVAGSQWFLSGNGSEYIVDLNDGQLEFYTATQVTIAAGQFEMNLEHSFL EIKFIDLTYSQSWQYDVHINYTEQVNLGLKTVTTSTGATKQIFNFTQSVR NMTVDVTKTQAEITFEIVMGAVTASLALVAVLGPIVDGLASAAEVTVES VEEGSAVINETTFVEELSGSDEAEEQNLANEKDALANGAEQTAGRMTRI KNAFNSTRWKVFGGITGAVAAASGIEIAVSAIMAAVYNNEWDNVPGFDE FANDAIEPYTFPGVTGYDLTSAWLADSLQIGLKTK
Ps_4943	MRMAKTLQQRLDQANCDYDIISHPHSATSLESARTAGVPAERVAKSVML DDRHGNYLMAVLPANRHLDMSKVRMTGAWQLTRESGLPTLFGDCERG AIPALGDAYDVKMLLDPSLTRQGDVYLEAGDHDHLIHMSMEQYLKLVP HAEVRELC
Ps_4451	MRKPPFLRSLLGLLALACSQAMAAPSPYSTLIVFGDSLSDAGQFPDLAGG TAAMRFTNRDTDGNYAPVSPMLLGGRLGVAPADLNPSTSLAVRPDGNN WAVGGYTTQQILDSITDTSRTVIPPGNPGAGAVLRERPGYLASGLGADPN ALYYLTGGGNDFLQGLVNSPADAAAAGARLAASAQALQQGGARYIMV WLLPDLGQTPNFSGTPQQGPLSQLSGVFNQSLVEQLDRVDAEIIPLNIPVL LQEALASPAQFGLAADQDLVGTCYSGGSCVENPVYGINGPTPDPSRLLFN DSVHPTIAGQRLIADYAYSIIAAPWELTLLPEMAHASLRAHQDELRNQW QTPWQAVGQWQAILATGAQDLDFDDQRSAASGDGRGYNLTLGGSYRL DEAWRIGLAAGVYRQKLEAGEQDSDYKLDSYLATLFAQFRQQRWWAD AALTAGHLDYHDLERTFALGVGERSEKGDTDGETWALSGRLGYNLATE GSDWQLSPFVSADYARVKVDGYDEKSGRSTALGFDDQDRTSRRLGVGL QGSYLFAPGTRLFAEVAREHEFEDDRQDLTMRLATLPANDFTLTGYTPH SNLTRASLGLTHELTPGLHVRGNYNWRKSDELTQQGVSLALSLDF
Ps_1958	MDIDELLKDLLGPGFKSLDGFCQLLKVDRDKLLKFLYKRKGSHYVSFSIL KKNKTHRSIKAPKRVMKKIQHALLPHLEKFYSPKPSSHGFVKGRSVKTN AQIHSRKRYVFNIDLKDFFESIHFGRVRNLFMAPPFDAAYNVATVMAHIC CSDGKLAQGAPTSPLISNMICRKLDSQLQALAKSCKCHFTRYADDITFSF TTTAKYLPKDIVEVSEDGRAIPGRELEEIIKSNGFIINSEKTRLQHRTQRQM VTGLVVNEMPNVTREFIRLTSSMINALNRYGPEMAEAKYLEILKGENQPL QPRKILRTKENAGDFFIKVVKGRLNYIQMIRGRGDKIYRRLAYEFTVAIG KENPEFKKSPEEILGNSIFVVNNIIDESQGTAFLLDGVGIVTNEHVVTGVS KTIARHSISFKRAGDTREYSADLILSDKKADLAIFHPNEEFRNIPALRKSDK TIVRPTDPVLSIGFPRHRDGAAHYIAKGHTTQRRRQVDLDLWLVDFTLM

	EGNSGGPMFNDSMEVIGVTARGAKNNIDAALYGFIPLESLNSFINRADFL LLKRLYDYLGNGSLNLLPRVPGKGVFSSTYQTKLHKEHLQKAKAV
Ps_3046	MRVWWLSAGLALFCLAQGAAAGTLLVVGDSISAGFGLDSRQGWVALL QQRLEEEGYDDQVVNASISGDTSAGGQARLPALLAEHKPSLVVLELGGN DGLRGQPPEQLQQNLASMIDRSRDAGAKVVLLGMRLPPNYGVRYTTAF AQVYEQLAAQKQVPLVPFFLEGVGGVAQMMQADGIHPAQGAQQRLLE NAWPAIKPLL
Ps_535	MNQDLATRYPLVLVPGMLGFVRVLLYPYWYGIVPALRRGGAQVFPVQV SPLHASEVRGEQLLAIIEDICRRTGAERVNLIGHSQGALSARYAAAKRPD RVASVTSVAGPNQGSELADYLAHKAPGDSPQGRILKAVLHGLAVLLVW LETGWRREPLPIDVHASHQSLTSAGVALFNQAYPQGLPTSWGGEGPAEV DGVRYYSWSGTLQPGRTDQGRNRFDGSNRFCRLFARTFTREKGQCDGM VGRYSSHLGQVIGDDYPLDHLDIVNQSLGAVGKGADPVRLFTEHAARLK AAGL
Rh_477	VILVVAGLLVAAPASSAAPPPDWKYTMVAFSNASDRDMDVYESVDGTG FQLVQQSAYRPPSGLVRDPSIFRNTDGLYYLTYTTGGGANIGFARSSDRIN WTPLGNYPVPFCCALMPGTGDGTGSASPPGFSGSAGFSDGPSLSPFVTKA WAPEWFVDGDRVNVILSMSTGGGFVPYLMTALEPSLRLWSPPVPLAGIG ADHIDTTVVKVGSTYHAFTKNETRKVVEHAVAPSVTGPYSFVPPGNWGS LVEGPAVVQLPSGDWRIYLDAYTEGKYLYSDSTDGLNTWSPVQEVPGVS GTARHLGIMREPA
Rh_2293	MENQDRGSARTSRRQFISVAGLAATAVITLATSSTASAAGPTAPNPGSRV GDPAEAQAVQRVAETLLNSGVPGLAFAIVKPDEKNRKASVTTTYHYGQ ADVENGVRVTPRTQFEIASETKTFTAALLAKLIARGEVGLDDLASKYSDG NPLPKGSGGEEITLRQLVTHRSGLSDDPPNLSAGCADPTQSCVDEKAKYT RDILWEGLRAPGALEFAPGSHWLYSDFGFGLLGTLMADKIIPGQEKPPFA AAVAREITDPLGMMGTVIETKATDLAVPYYLDGTRAPLWNNTGAIAGG GGLVSTAEDMSIWAATTLGYGNNPLKPVLTSMLEQIDTQAPENPAFGMG MAWQLQPPTPNFPQRFAKKNGDSSGSNCITLLVPDSGWSITILANGGNAA MIDPAAVNLMHDLVPRRPIFGSSTGSSSGSDAGFQTGSFG
Rh_4826	VLPRAETTPTKDGCMKKSTLRTGTVAALLTGSVLLLSAAPASADPGSLGS GGSSGSSGSLGSAGSISSGSAALPIPSPAGLIALAAASTQTGKPYQWGGVG PNSWDCSGLVQWAFRQAGVNLPRTSQQQANVGQPVPRWALAPGDVITF YPGATHVGIYAGFGMVFNAYGVGVPTGLTPLADLPINNIRRF
PueB	MSMSIFDYKTALGGDGKALYSEAITLALYASTPTGEALPGTAWRPISVSQ LGYQGNVSAQGTISGEQAIVSDAQSRCWANTTRPGSCCPSASSFRGTRQP QGRYQRLAGGLRVGLLPTTTSRLAFDNLLGKVAAFAAAQGLSGSDVLV TGHSLGGLGGQPRGGHEQRSLGRLLPGRQLLGFASPTQSANSSQVLNIGY ETTRCSAPWTALISTALSLGTHWQAPGVATNNIVSFTDHYSSFLGEVDSP EHPQSAVLVGPQCGGLRRGLNRLINSDFYDLTSRDSTVVISNLSEGKRDQ VWVKDLNLYAEKHTGSTFIIGTQSNDLLHGGKGNDYLDGGAGDDRFRD DGGYNIIHGGQGHNVLELQQPLKNFSIANDGDGTLYIRDAYGGISMTRD VGALVSHETGSWWQLFGKDVSHSVTADGLQNGNQWTAYNHSLNGDA YGNALVASVDGDWLFGHGGDDLLSSDKANVTFVGGTGNDVMHSSGGG GNTFLFSGNFGFDLIHGYQNTDKLVFMGVPGVDAHYDYSQHLSQNGND TLVQVFGEFLRVNPWWGSAWTSLSGSGLVFA

Table A3: List of primers and thermocycler conditions.

Amplification of Rh_4826 Forward primer: ATGCTGCCGCGC Reverse primer: CTAGAACCTGCGGATGT Thermocycler protocol: Initial Denaturation – 95°C, 60 s Repeat 30x Denaturation – 95°C, 30 s Annealing – ramp temperature from 50°C to 62°C at 0.4°C/s (30 s total) Extension – 72°C, 90 s Final Extension – 72°C, 300 s Idle – 4°C
Addition of Overlaps to Rh_4826 Forward primer: CTTTAAGAAGGAGATATACCATGCTGCCGCGC Reverse primer: GAACCTGCGGATGTGATGATGGTGATGCGAAGATCC Thermocycler protocol: Initial Denaturation – 95°C, 60 s Repeat 10x Denaturation – 95°C, 30 s Annealing – ramp temperature from 50°C to 62°C at 0.4°C/s (30 s total) Extension – 72°C, 90 s Repeat 25x Denaturation – 95°C, 30 s Annealing – 69°C, 30 s Extension – 72°C, 90 s Final Extension – 72°C, 300 s Idle – 4°C
Linearization of pET vector Forward primer: CGCATCACCATCATCACCATTAGTGATGAACTGAGATC Reverse primer: GGTATATCTCCTTCTTAAAGTTAAACAAAATTATTTCTAGAGGGG Thermocycler protocol: Initial Denaturation – 98°C, 30 s Repeat 25x Denaturation – 98°C, 10 s Annealing – 55°C, 15 s Extension – 72°C, 210 s Final Extension – 72°C, 300 s Idle – 4°C
Sequencing of Rh_4826 Forward primer: ATGCTGCCGCGC Reverse primer: CTAGAACCTGCGGATGT
Sequencing of pET_Rh_4826 Forward primer (T7 Promoter): TAATACGACTCACTATAGGG Reverse primer (T7 Terminator): GCTAGTTATTGCTCAGCGG

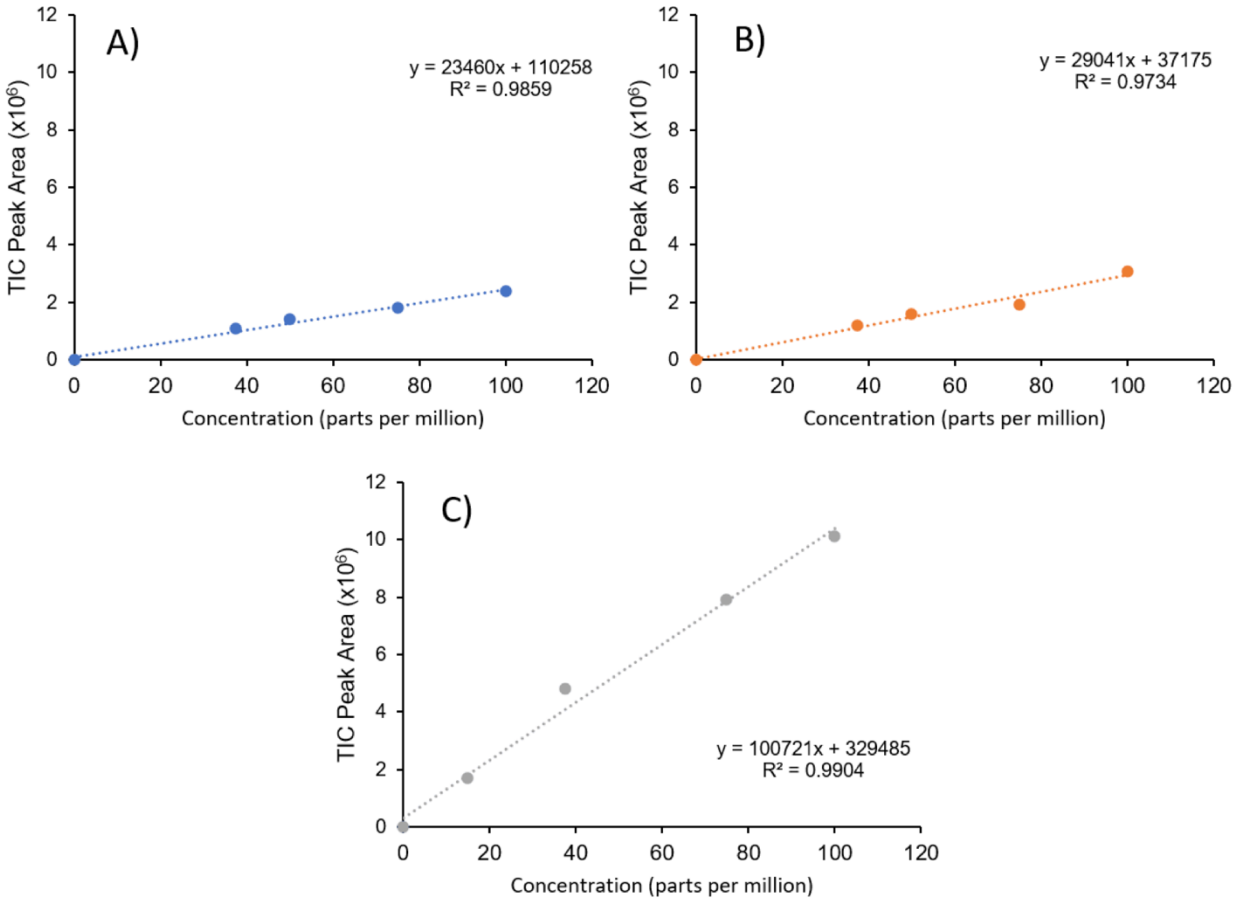

Figure A2: Calibration curves of A) diol 1, B) diol 2, and C) diacid 1 used to determine the concentration of products in the *Pseudomonas sp.* cholesterol esterase–degraded PU foam particulates. Standards were prepared by dissolving the diols and diacid in PBS media and performing the EtOAc extraction and GCMS analysis described in Section 4.3. All standards and samples were integrated using the ChemStation software integration tool.

REFERENCES

AAT Bioquest, Inc. 2021. PBS (Phosphate Buffered Saline) (1X, pH 7.4). https://www.aatbio.com/resources/buffer-preparations-and-recipes/pbs-phosphate-buffered-saline.

Akutsu-Shigeno, Yukie, Yusuke Adachi, Chise Yamada, Kieko Toyoshima, Nobuhiko Nomura, Hiroo Uchiyama, and Toshiaki Nakajima-Kambe. 2006. "Isolation of a bacterium that degrades urethane compounds and characterization of its urethane hydrolase." *Applied Microbiology and Biotechnology* 70 (4): 422-429. https://doi.org/10.1007/s00253-005-0071-1.

Ali, Sameh S., Tamer Elsamahy, Rania Al-Tohamy, Daochen Zhu, Yehia A. G. Mahmoud, Eleni Koutra, Metwally A. Metwally, Michael Kornaros, and Jianzhong Sun. 2021. "Plastic wastes biodegradation: Mechanisms, challenges and future prospects." *Science of The Total Environment* 780: 146590. https://doi.org/10.1016/j.scitotenv.2021.146590.

Altschul, S. F., T. L. Madden, A. A. Schäffer, J. Zhang, Z. Zhang, W. Miller, and D. J. Lipman. 1997. "Gapped BLAST and PSI-BLAST: a new generation of protein database search programs." *Nucleic acids research* 25 (17): 3389-3402. https://doi.org/10.1093/nar/25.17.3389.

Altschul, Stephen F., John C. Wootton, E. Michael Gertz, Richa Agarwala, Aleksandr Morgulis, Alejandro A. Schäffer, and Yi-Kuo Yu. 2005. "Protein database searches using compositionally adjusted substitution matrices." *The FEBS journal* 272 (20): 5101-5109. https://doi.org/10.1111/j.1742-4658.2005.04945.x.

Amobonye, Ayodeji, Prashant Bhagwat, Suren Singh, and Santhosh Pillai. 2021. "Plastic biodegradation: Frontline microbes and their enzymes." *Science of The Total Environment* 759: 143536. https://doi.org/10.1016/j.scitotenv.2020.143536.

Anbumani, Sadasivam, and Poonam Kakkar. 2018. "Ecotoxicological effects of microplastics on biota: a review." *Environmental Science and Pollution Research* 25 (15): 14373-14396. https://doi.org/10.1007/s11356-018-1999-x.

Anderson, Guillermo, and Noa Shenkar. 2021. "Potential effects of biodegradable single-use items in the sea: Polylactic acid (PLA) and solitary ascidians." *Environmental Pollution* 268: 115364. https://doi.org/10.1016/j.envpol.2020.115364.

Andrady, Anthony L. 2017. "The plastic in microplastics: A review." *Marine Pollution Bulletin* 119 (1): 12-22. https://doi.org/10.1016/j.marpolbul.2017.01.082.

Apprill, A., S. McNally, R. Parsons, and L. Weber. 2015. "Minor revision to V4 region SSU rRNA 806R gene primer greatly increases detection of SAR11 bacterioplankton." *Aquatic Microbial Ecology* 75 (2): 129-137. http://www.int-res.com/abstracts/ame/v75/n2/p129-137/.

Asaro, Lucia, Michel Gratton, Saïd Seghar, and Nourredine Aït Hocine. 2018. "Recycling of rubber wastes by devulcanization." *Resources, Conservation and Recycling* 133: 250-262. https://doi.org/10.1016/j.resconrec.2018.02.016.

Azoulay, David, Priscilla Villa, Yvette Arellano, Miriam Gordon, Doun Moon, Kathryn Miller, and Kristen Thompson. 2019. Plastic & Health: The Hidden Costs of a Plastic Planet. https://www.ciel.org/wp-content/uploads/2019/02/Plastic-and-Health-The-Hidden-Costs-of-a-Plastic-Planet-February-2019.pdf.

Bankevich, Anton, Sergey Nurk, Dmitry Antipov, Alexey A. Gurevich, Mikhail Dvorkin, Alexander S. Kulikov, Valery M. Lesin, Sergey I. Nikolenko, Son Pham, Andrey D. Prjibelski, Alexey V. Pyshkin, Alexander V. Sirotkin, Nikolay Vyahhi, Glenn Tesler, Max A. Alekseyev, and Pavel A. Pevzner. 2012. "SPAdes: A New Genome Assembly Algorithm and Its Applications to Single-Cell Sequencing." *Journal of Computational Biology* 19 (5): 455-477. https://doi.org/10.1089/cmb.2012.0021.

bcl2fastq2 Conversion Software v2.20. 2019. https://support.illumina.com/sequencing/sequencing_software/bcl2fastq-conversion-software.html.

Besemer, John, Alexandre Lomsadze, and Mark Borodovsky. 2001. "GeneMarkS: a self-training method for prediction of gene starts in microbial genomes. Implications for finding sequence motifs in regulatory regions." *Nucleic Acids Research* 29 (12): 2607-2618. https://doi.org/10.1093/nar/29.12.2607.

Besser, J., H. A. Carleton, P. Gerner-Smidt, R. L. Lindsey, and E. Trees. 2018. "Next-generation sequencing technologies and their application to the study and control of bacterial infections." *Clinical Microbiology and Infection* 24 (4): 335-341. https://doi.org/https://doi.org/10.1016/j.cmi.2017.10.013.

Betts, Kellyn. 2008. "Why small plastic particles may pose a big problem in the oceans." *Environmental Science & Technology* 42 (24): 8995-8995. https://doi.org/10.1021/es802970v.

Biffinger, Justin C., Daniel E. Barlow, Allison L. Cockrell, Kathleen D. Cusick, William J. Hervey, Lisa A. Fitzgerald, Lloyd J. Nadeau, Chia S. Hung, Wendy J. Crookes-Goodson, and John N. Russell. 2015. "The applicability of Impranil®DLN for gauging the biodegradation of polyurethanes." *Polymer Degradation and Stability* 120: 178-185. https://doi.org/10.1016/j.polymdegradstab.2015.06.020.

Bolivar, Francisco, Raymond L. Rodriguez, Patricia J. Greene, Mary C. Betlach, Herbert L. Heyneker, Herbert W. Boyer, Jorge H. Crosa, and Stanley Falkow. 1977. "Construction and characterization of new cloning vehicle. II. A multipurpose cloning system." *Gene* 2 (2): 95-113. https://doi.org/10.1016/0378-1119(77)90000-2. https://www.sciencedirect.com/science/article/pii/0378111977900002.

Böhlen, Peter, Stanley Stein, Wallace Dairman, and Sidney Udenfriend. 1973. "Fluorometric assay of proteins in the nanogram range." *Archives of Biochemistry and Biophysics* 155 (1): 213-220. https://doi.org/10.1016/S0003-9861(73)80023-2. https://www.sciencedirect.com/science/article/pii/S0003986173800232.

Das, Kishore, and Ashis K. Mukherjee. 2007. "Crude petroleum-oil biodegradation efficiency of Bacillus subtilis and Pseudomonas aeruginosa strains isolated from a petroleum-oil contaminated soil from North-East India." *Bioresource Technology* 98 (7): 1339-1345. https://doi.org/10.1016/j.biortech.2006.05.032.

do Canto, Vanessa Petry, Claudia Elizabeth Thompson, and Paulo Augusto Netz. 2019. "Polyurethanases: Three-dimensional structures and molecular dynamics simulations of enzymes that degrade polyurethane." *Journal of Molecular Graphics and Modelling* 89: 82-95. https://doi.org/10.1016/j.jmgm.2019.03.001.

Doddamani, Hanumanthanaik P., and Harichandra Z. Ninnekar. 2001. "Biodegradation of Carbaryl by a Micrococcus Species." *Current Microbiology* 43 (1): 69-73. https://doi.org/10.1007/s002840010262.

Domańska, Magdalena, Kamila Hamal, Bartosz Jasionowski, and Janusz Łomotowski. 2019. "Bacteriological Contamination Detection in Water and Wastewater Samples Using OD600." *Polish Journal of Environmental Studies* 28 (6): 4503-4509. https://doi.org/10.15244/pjoes/94838.

Dovichi, Norman J. 1997. "DNA sequencing by capillary electrophoresis." *ELECTROPHORESIS* 18 (12-13): 2393-2399. https://doi.org/10.1002/elps.1150181229.

Dubendorff, John W., and F. William Studier. 1991. "Controlling basal expression in an inducible T7 expression system by blocking the target T7 promoter with lac repressor." *Journal of Molecular Biology* 219 (1): 45-59. https://doi.org/10.1016/0022-2836(91)90856-2.

Elizaquível, P., and R. Aznar. 2008. "Comparison of Four Commercial DNA Extraction Kits for PCR Detection of Listeria monocytogenes, Salmonella, Escherichia coli O157:H7, and Staphylococcus aureus in Fresh, Minimally Processed Vegetables." *Journal of Food Protection* 71 (10): 2110-2114. https://doi.org/10.4315/0362-028X-71.10.2110.

Eriksen, M. K., J. D. Christiansen, A. E. Daugaard, and T. F. Astrup. 2019. "Closing the loop for PET, PE and PP waste from households: Influence of material properties and product design for plastic recycling." *Waste Management* 96: 75-85. https://doi.org/10.1016/j.wasman.2019.07.005.

Espinosa, María José Cárdenas, Andrea Colina Blanco, Tabea Schmidgall, Anna Katharina Atanasoff-Kardjalieff, Uwe Kappelmeyer, Dirk Tischler, Dietmar H. Pieper, Hermann J. Heipieper, and Christian Eberlein. 2020. "Toward Biorecycling: Isolation of a Soil

Bacterium That Grows on a Polyurethane Oligomer and Monomer." *Frontiers in Microbiology* 11: 404. https://www.frontiersin.org/article/10.3389/fmicb.2020.00404.

Gamerith, Caroline, Enrique Herrero Acero, Alessandro Pellis, Andreas Ortner, Robert Vielnascher, Daniel Luschnig, Barbara Zartl, Karolina Haernvall, Sabine Zitzenbacher, Gernot Strohmeier, Oskar Hoff, Georg Steinkellner, Karl Gruber, Doris Ribitsch, and Georg M. Guebitz. 2016. "Improving enzymatic polyurethane hydrolysis by tuning enzyme sorption." *Polymer Degradation and Stability* 132: 69-77. https://doi.org/10.1016/j.polymdegradstab.2016.02.025.

Gan, Zhiqiang, and Houjin Zhang. 2019. "PMBD: a Comprehensive Plastics Microbial Biodegradation Database." *Database* 2019. https://doi.org/10.1093/database/baz119.

Gardes, M., and T. D. Bruns. 1993. "ITS primers with enhanced specificity for basidiomycetes - application to the identification of mycorrhizae and rusts." *Molecular Ecology* 2 (2): 113-118. https://doi.org/10.1111/j.1365-294X.1993.tb00005.x.

Gautam, Rajeeb, Amarjeet S. Bassi, and Ernest K. Yanful. 2007. "Candida rugosa lipase-catalyzed polyurethane degradation in aqueous medium." *Biotechnology Letters* 29 (7): 1081-1086. https://doi.org/10.1007/s10529-007-9354-1.

Geyer, Roland, Jenna R. Jambeck, and Kara Lavender Law. 2017. "Production, use, and fate of all plastics ever made." *Science Advances* 3 (7): e1700782. https://doi.org/10.1126/sciadv.1700782.

Gu, Ji-Dong, and Ralph Mitchell. 2004. "Degradation of Polyurethane by Bacterium Isolated from Soil." https://onepetro.org/NACECORR/proceedings-abstract/CORR04/All-CORR04/NACE-04584/115843.

Gunawan, Natasha R., Marissa Tessman, Ariel C. Schreiman, Ryan Simkovsky, Anton A. Samoylov, Nitin K. Neelakantan, Troy A. Bemis, Michael D. Burkart, Robert S. Pomeroy, and Stephen P. Mayfield. 2020. "Rapid biodegradation of renewable polyurethane foams with identification of associated microorganisms and decomposition products." *Bioresource Technology Reports* 11: 100513. https://doi.org/10.1016/j.biteb.2020.100513.

Gurevich, Alexey, Vladislav Saveliev, Nikolay Vyahhi, and Glenn Tesler. 2013. "QUAST: quality assessment tool for genome assemblies." *Bioinformatics (Oxford, England)* 29 (8): 1072-1075. https://doi.org/10.1093/bioinformatics/btt086.

Howard, Gary T. 2002. "Biodegradation of polyurethane: a review." *International Biodeterioration & Biodegradation* 49 (4): 245-252. https://doi.org/10.1016/S0964-8305(02)00051-3.

Howard, Gary T., Brian Crother, and Jared Vicknair. 2001. "Cloning, nucleotide sequencing and characterization of a polyurethanase gene (pueB) from Pseudomonas chlororaphis."

International Biodeterioration & Biodegradation 47 (3): 141-149. https://doi.org/10.1016/S0964-8305(01)00042-7.

Hubálek, Zdenek. 2003. "Protectants used in the cryopreservation of microorganisms." *Cryobiology* 46 (3): 205-229. https://doi.org/10.1016/S0011-2240(03)00046-4.

Hunt, Martin, Nishadi De Silva, Thomas D. Otto, Julian Parkhill, Jacqueline A. Keane, and Simon R. Harris. 2015. "Circlator: automated circularization of genome assemblies using long sequencing reads." *Genome Biology* 16 (1): 294. https://doi.org/10.1186/s13059-015-0849-0.

Hyatt, Doug, Gwo-Liang Chen, Philip F. LoCascio, Miriam L. Land, Frank W. Larimer, and Loren J. Hauser. 2010. "Prodigal: prokaryotic gene recognition and translation initiation site identification." *BMC Bioinformatics* 11 (1): 119. https://doi.org/10.1186/1471-2105-11-119.

Iwata, Tadahisa. 2015. "Biodegradable and Bio-Based Polymers: Future Prospects of Eco-Friendly Plastics." *Angewandte Chemie International Edition* 54 (11): 3210-3215. https://doi.org/10.1002/anie.201410770.

Katoh, Kazutaka, and Daron M. Standley. 2013. "MAFFT Multiple Sequence Alignment Software Version 7: Improvements in Performance and Usability." *Molecular Biology and Evolution* 30 (4): 772-780. https://doi.org/10.1093/molbev/mst010.

Kurtz, Stefan, Adam Phillippy, Arthur L. Delcher, Michael Smoot, Martin Shumway, Corina Antonescu, and Steven L. Salzberg. 2004. "Versatile and open software for comparing large genomes." *Genome Biology* 5 (2): R12. https://doi.org/10.1186/gb-2004-5-2-r12.

Lander, Eric S., and Michael S. Waterman. 1988. "Genomic mapping by fingerprinting random clones: A mathematical analysis." *Genomics* 2 (3): 231-239. https://doi.org/https://doi.org/10.1016/0888-7543(88)90007-9.

Li, Heng. 2013. "Aligning sequence reads, clone sequences and assembly contigs with BWA-MEM." *arXiv preprint arXiv:1303.3997*. https://arxiv.org/pdf/1303.3997v2.pdf.

Li, Heng, Bob Handsaker, Alec Wysoker, Tim Fennell, Jue Ruan, Nils Homer, Gabor Marth, Goncalo Abecasis, Richard Durbin, and Subgroup Genome Project Data Processing. 2009. "The Sequence Alignment/Map format and SAMtools." *Bioinformatics* 25 (16): 2078-2079. https://doi.org/10.1093/bioinformatics/btp352.

Litfin, Thomas, Yaoqi Zhou, and Yuedong Yang. 2017. "SPOT-ligand 2: improving structure-based virtual screening by binding-homology search on an expanded structural template library." *Bioinformatics* 33 (8): 1238-1240. https://doi.org/10.1093/bioinformatics/btw829.

Lu, Xiaoxia, Nandi Zhou, and Yaping Tian. 2015. "Spectrophotometric determination of ethyl carbamate through bi-enzymatic cascade reactions." *Analytical Methods* 7 (4): 1261-1264. https://doi.org/10.1039/C4AY02693D.

Magnin, Audrey, Eric Pollet, Luc Avérous, Gert Weber, Uwe T. Bornscheuer, and Ren Wei. 2021. "Chapter Fifteen - Characterization of the enzymatic degradation of polyurethanes." In *Methods in Enzymology*, 317-336. Academic Press. https://doi.org/10.1016/bs.mie.2020.12.011.

Magnin, Audrey, Eric Pollet, Rémi Perrin, Christophe Ullmann, Cécile Persillon, Vincent Phalip, and Luc Avérous. 2019. "Enzymatic recycling of thermoplastic polyurethanes: Synergistic effect of an esterase and an amidase and recovery of building blocks." *Waste Management* 85: 141-150. https://doi.org/https://doi.org/10.1016/j.wasman.2018.12.024.

Mardis, E., and W. R. McCombie. 2017. "Library Quantification: Fluorometric Quantitation of Double-Stranded or Single-Stranded DNA Samples Using the Qubit System." *Cold Spring Harb Protoc* 2017 (6): pdb.prot094730. https://doi.org/10.1101/pdb.prot094730.

Masaki, Kazuo, Kanako Fujihara, Dararat Kakizono, Taichi Mizukure, Masaki Okuda, and Nobuhiko Mukai. 2020. "Aspergillus oryzae acetamidase catalyzes degradation of ethyl carbamate." *Journal of Bioscience and Bioengineering* 130 (6): 577-581. https://doi.org/https://doi.org/10.1016/j.jbiosc.2020.07.015.

Masnadi, Mohammad S., Hassan M. El-Houjeiri, Dominik Schunack, Yunpo Li, Jacob G. Englander, Alhassan Badahdah, Jean-Christophe Monfort, James E. Anderson, Timothy J. Wallington, Joule A. Bergerson, Deborah Gordon, Jonathan Koomey, Steven Przesmitzki, Inês L. Azevedo, Xiaotao T. Bi, James E. Duffy, Garvin A. Heath, Gregory A. Keoleian, Christophe McGlade, D. Nathan Meehan, Sonia Yeh, Fengqi You, Michael Wang, and Adam R. Brandt. 2018. "Global carbon intensity of crude oil production." *Science* 361 (6405): 851. https://doi.org/10.1126/science.aar6859.

McLeod, Michael P., René L. Warren, William W. L. Hsiao, Naoto Araki, Matthew Myhre, Clinton Fernandes, Daisuke Miyazawa, Wendy Wong, Anita L. Lillquist, Dennis Wang, Manisha Dosanjh, Hirofumi Hara, Anca Petrescu, Ryan D. Morin, George Yang, Jeff M. Stott, Jacqueline E. Schein, Heesun Shin, Duane Smailus, Asim S. Siddiqui, Marco A. Marra, Steven J. M. Jones, Robert Holt, Fiona S. L. Brinkman, Keisuke Miyauchi, Masao Fukuda, Julian E. Davies, William W. Mohn, and Lindsay D. Eltis. 2006. "The complete genome of Rhodococcus sp. RHA1 provides insights into a catabolic powerhouse." *Proceedings of the National Academy of Sciences* 103 (42): 15582. https://doi.org/10.1073/pnas.0607048103.

Moore, Charles James. 2008. "Synthetic polymers in the marine environment: A rapidly increasing, long-term threat." *Environmental Research* 108 (2): 131-139. https://doi.org/https://doi.org/10.1016/j.envres.2008.07.025.

Nguyen, Huu Tam, Girish Mishra, Edward Whittle, Mark S. Pidkowich, Scott A. Bevan, Ann Owens Merlo, Terence A. Walsh, and John Shanklin. 2010. "Metabolic Engineering of Seeds Can Achieve Levels of ω-7 Fatty Acids Comparable with the Highest Levels Found in Natural Plant Sources." *Plant Physiology* 154 (4): 1897-1904. https://doi.org/10.1104/pp.110.165340.

Osman, Muhammad, Sadia Mehmood Satti, Aaisha Luqman, Fariha Hasan, Ziaullah Shah, and Aamer Ali Shah. 2018. "Degradation of Polyester Polyurethane by Aspergillus sp. Strain S45 Isolated from Soil." *Journal of Polymers and the Environment* 26 (1): 301-310. https://doi.org/10.1007/s10924-017-0954-0.

Otzen, Marleen, Cyntia Palacio, and Dick B. Janssen. 2018. "Characterization of the caprolactam degradation pathway in Pseudomonas jessenii using mass spectrometry-based proteomics." *Applied Microbiology and Biotechnology* 102 (15): 6699-6711. https://doi.org/10.1007/s00253-018-9073-7.

Parada, Alma E., David M. Needham, and Jed A. Fuhrman. 2016. "Every base matters: assessing small subunit rRNA primers for marine microbiomes with mock communities, time series and global field samples." *Environmental Microbiology* 18 (5): 1403-1414. https://doi.org/10.1111/1462-2920.13023.

Peng, Yu-Huei, Yang-hsin Shih, Yen-Chun Lai, Yuan-Zan Liu, Ying-Tong Liu, and Nai-Chun Lin. 2014. "Degradation of polyurethane by bacterium isolated from soil and assessment of polyurethanolytic activity of a Pseudomonas putida strain." *Environmental Science and Pollution Research* 21 (16): 9529-9537. https://doi.org/10.1007/s11356-014-2647-8.

Pradhan, Ranjan, Manjusri Misra, Larry Erickson, and Amar Mohanty. 2010. "Compostability and biodegradation study of PLA–wheat straw and PLA–soy straw based green composites in simulated composting bioreactor." *Bioresource Technology* 101 (21): 8489-8491. https://doi.org/10.1016/j.biortech.2010.06.053.

Rodriguez-R, Luis M., Santosh Gunturu, William T. Harvey, Ramon Rosselló-Mora, James M. Tiedje, James R. Cole, and Konstantinos T. Konstantinidis. 2018. "The Microbial Genomes Atlas (MiGA) webserver: taxonomic and gene diversity analysis of Archaea and Bacteria at the whole genome level." *Nucleic Acids Research* 46 (W1): W282-W288. https://doi.org/10.1093/nar/gky467.

Rowe, Lori, and Gary T. Howard. 2002. "Growth of Bacillus subtilis on polyurethane and the purification and characterization of a polyurethanase-lipase enzyme." *International Biodeterioration & Biodegradation* 50 (1): 33-40. https://doi.org/10.1016/S0964-8305(02)00047-1.

Roy, Ambrish, Alper Kucukural, and Yang Zhang. 2010. "I-TASSER: a unified platform for automated protein structure and function prediction." *Nature protocols* 5 (4): 725-738. https://doi.org/10.1038/nprot.2010.5.

Saladi, Shyam M. 2018. smsaladi/genome_size_vs_protein_count: Genome size vs. protein count, a Shiny app. CaltechDATA. http://dx.doi.org/10.22002/D1.1093.

Santerre, J. P., and R. S. Labow. 1997. "The effect of hard segment size on the hydrolytic stability of polyether-urea-urethanes when exposed to cholesterol esterase." *Journal of Biomedical Materials Research* 36 (2): 223-232. https://doi.org/10.1002/(SICI)1097-4636(199708)36:2<223::AID-JBM11>3.0.CO;2-H.

Schubert, Olga T., Hannes L. Röst, Ben C. Collins, George Rosenberger, and Ruedi Aebersold. 2017. "Quantitative proteomics: challenges and opportunities in basic and applied research." *Nature Protocols* 12 (7): 1289-1294. https://doi.org/10.1038/nprot.2017.040.

Sheel, Anvita, Deepak Pant, Sabu Thomas, Ajay Vasudeo Rane, Krishnan Kanny, Abitha V.K, and Martin George Thomas. 2018. "6 - Chemical Depolymerization of Polyurethane Foams via Glycolysis and Hydrolysis." In *Recycling of Polyurethane Foams*, 67-75. William Andrew Publishing. https://doi.org/10.1016/B978-0-323-51133-9.00006-1.

Shilling, Patrick J., Kiavash Mirzadeh, Alister J. Cumming, Magnus Widesheim, Zoe Köck, and Daniel O. Daley. 2020. "Improved designs for pET expression plasmids increase protein production yield in Escherichia coli." *Communications Biology* 3 (1): 214. https://doi.org/10.1038/s42003-020-0939-8.

Sonnenschein, M.F. 2021. *Polyurethanes: Science, Technology, Markets, and Trends*. Wiley.

Stamps, Blake W., Sandra Zingarelli, Chia-Suei Hung, Carrie A. Drake, Vanessa A. Varaljay, Bradley S. Stevenson, and Wendy J. Crookes-Goodson. 2018. "Finished Genome Sequence of a Polyurethane-Degrading Pseudomonas Isolate." *Genome announcements* 6 (9): e00084-18. https://doi.org/10.1128/genomeA.00084-18.

Sun, Pingping, Amgad Elgowainy, Michael Wang, Jeongwoo Han, and Robert J. Henderson. 2018. "Estimation of U.S. refinery water consumption and allocation to refinery products." *Fuel* 221: 542-557. https://doi.org/10.1016/j.fuel.2017.07.089.

Thiounn, Timmy, and Rhett C. Smith. 2020. "Advances and approaches for chemical recycling of plastic waste." *Journal of Polymer Science* 58 (10): 1347-1364. https://doi.org/10.1002/pol.20190261.

Tournier, V., C. M. Topham, A. Gilles, B. David, C. Folgoas, E. Moya-Leclair, E. Kamionka, M. L. Desrousseaux, H. Texier, S. Gavalda, M. Cot, E. Guémard, M. Dalibey, J. Nomme, G. Cioci, S. Barbe, M. Chateau, I. André, S. Duquesne, and A. Marty. 2020. "An engineered PET depolymerase to break down and recycle plastic bottles." *Nature* 580 (7802): 216-219. https://doi.org/10.1038/s41586-020-2149-4.

Tyers, Mike, and Matthias Mann. 2003. "From genomics to proteomics." *Nature* 422 (6928): 193-197. https://doi.org/10.1038/nature01510.

Wei, Ren, and Wolfgang Zimmermann. 2017. "Microbial enzymes for the recycling of recalcitrant petroleum-based plastics: how far are we?" *Microbial biotechnology* 10 (6): 1308-1322. https://doi.org/10.1111/1751-7915.12710.

Welle, Frank. 2011. "Twenty years of PET bottle to bottle recycling—An overview." *Resources, Conservation and Recycling* 55 (11): 865-875. https://doi.org/https://doi.org/10.1016/j.resconrec.2011.04.009.

White, T. J., T. Bruns, S. Lee, J. Taylor, Michael A. Innis, David H. Gelfand, John J. Sninsky, and Thomas J. White. 1990. "38 - AMPLIFICATION AND DIRECT SEQUENCING OF FUNGAL RIBOSOMAL RNA GENES FOR PHYLOGENETICS." In *PCR Protocols*, 315-322. San Diego: Academic Press. https://msafungi.org/wp-content/uploads/2019/03/February-2013-Inoculum.pdf.

Wick, Ryan. 2018. Porechop. https://github.com/rrwick/Porechop: GitHub.

Wick, Ryan R., Louise M. Judd, Claire L. Gorrie, and Kathryn E. Holt. 2017. "Unicycler: Resolving bacterial genome assemblies from short and long sequencing reads." *PLoS computational biology* 13 (6): e1005595-e1005595. https://doi.org/10.1371/journal.pcbi.1005595.

Wick, Ryan R., Mark B. Schultz, Justin Zobel, and Kathryn E. Holt. 2015. "Bandage: interactive visualization of de novo genome assemblies." *Bioinformatics* 31 (20): 3350-3352. https://doi.org/10.1093/bioinformatics/btv383.

Wu, Chao-Hsiung, Ching-Yuan Chang, Chien-Min Cheng, and Hung-Chang Huang. 2003. "Glycolysis of waste flexible polyurethane foam." *Polymer Degradation and Stability* 80 (1): 103-111. https://doi.org/10.1016/S0141-3910(02)00390-7.

Yang, Jianyi, Renxiang Yan, Ambrish Roy, Dong Xu, Jonathan Poisson, and Yang Zhang. 2015. "The I-TASSER Suite: protein structure and function prediction." *Nature methods* 12 (1): 7-8. https://doi.org/10.1038/nmeth.3213.

Yang, Jianyi, and Yang Zhang. 2015. "I-TASSER server: new development for protein structure and function predictions." *Nucleic Acids Research* 43 (W1): W174-W181. https://doi.org/10.1093/nar/gkv342.

Yang, Wenqing, Qingyin Dong, Shili Liu, Henghua Xie, Lili Liu, and Jinhui Li. 2012. "Recycling and Disposal Methods for Polyurethane Foam Wastes." *Procedia Environmental Sciences* 16: 167-175. https://doi.org/https://doi.org/10.1016/j.proenv.2012.10.023.

Yang, Yuedong, Jian Zhan, and Yaoqi Zhou. 2016. "SPOT-Ligand: Fast and effective structure-based virtual screening by binding homology search according to ligand and receptor similarity." *Journal of Computational Chemistry* 37 (18): 1734-1739. https://doi.org/10.1002/jcc.24380.

Yashchuk, O., F. S. Portillo, and E. B. Hermida. 2012. "Degradation of Polyethylene Film Samples Containing Oxo-Degradable Additives." *Procedia Materials Science* 1: 439-445. https://doi.org/10.1016/j.mspro.2012.06.059.

Zhang, Zheng, Scott Schwartz, Lukas Wagner, and Webb Miller. 2000. "A Greedy Algorithm for Aligning DNA Sequences." *Journal of Computational Biology* 7 (1-2): 203-214. https://doi.org/10.1089/10665270050081478.

Zumstein, Michael T., Ramani Narayan, Hans-Peter E. Kohler, Kristopher McNeill, and Michael Sander. 2019. "Dos and Do Nots When Assessing the Biodegradation of Plastics." *Environmental Science & Technology* 53 (17): 9967-9969. https://doi.org/10.1021/acs.est.9b04513.

Zumstein, Michael Thomas, Arno Schintlmeister, Taylor Frederick Nelson, Rebekka Baumgartner, Dagmar Woebken, Michael Wagner, Hans-Peter E. Kohler, Kristopher McNeill, and Michael Sander. 2018. "Biodegradation of synthetic polymers in soils: Tracking carbon into CO_2 and microbial biomass." *Science Advances* 4 (7): eaas9024. https://doi.org/10.1126/sciadv.aas9024.